Elsevier Editorial System(tm) for Energy Conversion and Management
Manuscript Draft

Manuscript Number: ECM-D-14-02296

Title: Numerical simulation and exergetic analysis of building ventilation solar chimneys

Article Type: Original research paper

Section/Category: 1. Energy Conservation and Efficient Utilization

Keywords: Solar chimney; CFD; energy; energy-efficient building; solar passive design

Corresponding Author: Mrs. María José Suárez López, Ph.D.

Corresponding Author's Institution: Universidad de Oviedo

First Author: María José Suárez López, Ph.D.

Order of Authors: María José Suárez López, Ph.D.; Ana María Blanco-Marigorta, Ph.D.; Antonio José Gutiérrez-Trashorras, Ph.D.; Jorge Pistono-Favero, Ph.D.; Eduardo Blanco-Marigorta, Ph.D.

Abstract: Solar chimneys are passive solar devices, which improve natural building ventilation. A detailed exergetic analysis has been developed in this work, both for general balance and specific variables. To apply this analysis, a three-dimensional CFD model has been built and validated with bibliographic experimental data. The values of the variables have been examined both inside and at the exit of the solar chimney, resulting in a detailed description of the inner phenomena and parameters influencing the exergetic efficiency. Apart from a deeper understanding of thermal and fluid-dynamic behaviour, this study suggests some qualitative improvements, although the numerical data show that solar chimneys as natural ventilation systems offer quite a small efficiency.

Suggested Reviewers: Silvia Soutullo Ph.D.
Researcher, Renewable Energy - Uie3, CIEMAT
silvia.soutullo@ciemat.es

Cristina Sanjuan Ph.D.
Researcher, ARUP
cristina.sanjuan@arup.com

Monia Galdo Ph.D.
Teacher, Energy, Universidad de Oviedo
galdomonica@uniovi.es

Cover letter

Dear Sirs

We enclose herewith the paper titled ***Numerical simulation and exergetic analysis of building ventilation solar chimneys*** submitted for publication in the journal **Energy Conversion and Management** according to the rules applied for authors; the authors acknowledge that the submission declaration has been properly complied with; all necessary permission have been obtained.

The ARFRISOL project (Bioclimatic Architecture and Solar Cooling) aim is to demonstrate the feasibility of bioclimatic systems and absorptive solar air conditioning in real buildings. One of these systems is the solar chimney, which has been the object of the research presented in this article.

This paper develops first a general exergetic analysis applied to solar chimneys used for building ventilation, defining the specific exergies, its balances and efficiencies. Afterwards a CFD tri-dimensional model has been generated to analyse the thermal and dynamic behavior of the fluid in a solar chimney. The results were validated with data available in the bibliography, obtaining a good correspondence. The values of the variables have been checked both inside and at the exit of the solar chimney, resulting in a detailed description of the inside phenomena and of the parameters influencing the exergetic efficiency.

We hope you find the article interesting and worthy of publication in the Journal.

Yours sincerely
María José Suárez López

Energy Conversion and Management
Submission Checklist

Please save a copy of this form to your computer, complete and upload as 'Checklist for New Submissions'.

Your manuscript will be considered incomplete unless all the below requirements have been met. Please initial each step to confirm.

(1) I María José Suárez-López confirm that the work described has not been published previously (except in the form of an abstract or as part of a published lecture or academic thesis), that it is not under consideration for publication elsewhere, that its publication is approved by all authors and that, if accepted, it will not be published elsewhere in the same form, in English or in any other language, without the written consent of the Publisher.

Authors found to be deliberately contravening the submission guidelines on originality and exclusivity shall not be considered for future publication in this journal.

(2) The source document is editable, i.e. Word, WordPerfect or Latex
MJ {enter initials}

(3) The source document is double-spaced
MJ {enter initials}

(4) The source document has been prepared prepared in 12 or 10 point font size, preferably 12 points
MJ {enter initials}

(5) The source document is in one column per page
MJ {enter initials}

(6) The figures and tables have been supplied: either integrated with the text file or as separate files.
MJ {enter initials}

Highlights:

- Exergetic analysis of a building ventilation solar chimney.
- Numerical CFD model developed, validated and employed to study the flow.
- Analysis of the solar chimney energy and exergy efficiencies.
- Mechanical and thermal exergy distributions have been analyzed.
- Crucial points in the chimney identified to improve its performance.

Numerical simulation and exergetic analysis of building ventilation solar chimneys

María José Suárez-López[a*], *Ana María Blanco-Marigorta*[b], *Antonio José Gutiérrez-Trashorras*[a], *Jorge Pistono-Favero*[a], *Eduardo Blanco-Marigorta*[a]

[a]*Universidad de Oviedo, EDZE (Energía), Campus de Viesques, 33203 Gijón (Asturias) Spain.*
[b]*Universidad de Las Palmas de Gran Canaria, Departamento de Ingeniería de Procesos, Edificio de Ingenierías-Tafira Baja, 35017 Las Palmas G.C. Spain*

[*]Corresponding author. Tel.: +34 985182366.
E-mail address: suarezlmaria@uniovi.es (M.J. Suárez).

Abstract

Solar chimneys are passive solar devices, which improve natural building ventilation. A detailed exergetic analysis has been developed in this work, both for general balance and specific variables. To apply this analysis, a three-dimensional CFD model has been built and validated with bibliographic experimental data. The values of the variables have been examined both inside and at the exit of the solar chimney, resulting in a detailed description of the inner phenomena and parameters influencing the exergetic efficiency. Apart from a deeper understanding of thermal and fluid-dynamic behaviour, this study suggests some qualitative improvements, although the numerical data show that solar chimneys as natural ventilation systems offer quite a small efficiency.

Keywords: Solar chimney, CFD, Exergy, Energy-efficient building, Solar passive design.

Nomenclature

$\dot{E}x$	exergy transfer rate (W)	Q	volumetric flow ($m^3\ s^{-1}$)
$\dot{E}x_G$	solar radiation exergy transfer rate (W)	ρ	density ($kg\ m^{-3}$)
$\dot{m}$	mass flow ($kg\ s^{-1}$)	φ	total exergetic efficiency
e	specific exergy ($J\ kg^{-1}$)	φ_u	useful exergetic efficiency
c_p	specific heat capacity ($J\ kg^{-1}\ K^{-1}$)	φ_{mec}	mechanical exergetic efficiency
T	temperature (K)	φ_{term}	thermal exergetic efficiency
T_S	solar radiation temperature (K)		
p	Pressure (Pa)	*Superscripts*	
z	height (m)	T	thermal
R	ideal gas constant ($J\ mol^{-1}\ K^{-1}$)	M	mechanical
v	velocity ($m\ s^{-1}$)		
g	gravitational acceleration ($m\ s^{-2}$)	*Subscripts*	
$\dot{W}_V$	ventilation power (W)	1	entrance
b	absorbing surface width (m)	2	exit
L	absorbing surface length (m)	D	destruction
G	solar radiation ($W\ m^{-2}$)	0	environment

1. **Introduction**

1.1. Description

Nowadays, due to the complex situation of the energy sector, there is a world agreement to promote energy savings techniques, particularly in the major consumption sectors. On that score, the final use of energy is usually classified in three main sectors: industry, transport and buildings. In developed countries as a whole, the buildings sector (which includes residential and commercial) is the final user of the biggest energy amount (35% to 45%) [1]. More than half of that energy is due to thermal conditioning. In order to reduce this percentage, there is a growing interest in the analysis of the buildings thermal performance and in the research of constructive solutions which can improve energy efficiency.

Solar radiation is one of the renewable energy sources with better prospects to soothe present energy troubles. The solar energy conversion into direct current electricity by photovoltaic effect has not achieved the expected performance yet, but the thermal use of solar radiation in buildings has already obtained good results. There are two kinds of methods to apply solar radiation in buildings: active and passive. Among the passive ones are the natural ventilation systems, which make use of solar radiation to generate convective flows helping ventilation and refreshing the inhabited areas. A building element specifically designed for that purpose is the solar chimney (Fig. 1), repeatedly used as a bioclimatic constructive element.

Fig. 1. CIEMAT research building at Almería's Solar Platform. Solar chimney detail.

One of the more efficient shapes of the solar chimney is an air channel with a parallelepiped form, where one of the vertical sides is made of glass and the others are opaque surfaces, which absorb solar radiation (Fig. 2). Air enters the chimney at its lower level from the premises which are to be ventilated. Solar radiation goes across glass and falls on the opaque surfaces; these opaque elements absorb most energy, increase its temperature and subsequently, hand over thermal energy to the air inside the chimney by natural convection. When this air is heated, its density decreases, generating a natural ascending flow; the air which reaches the open

top of the chimney is then evacuated to outside atmosphere. With a suitable insulation of the back of the absorbing wall it is easy to reduce the heat flow to the inside rooms to a minimum.

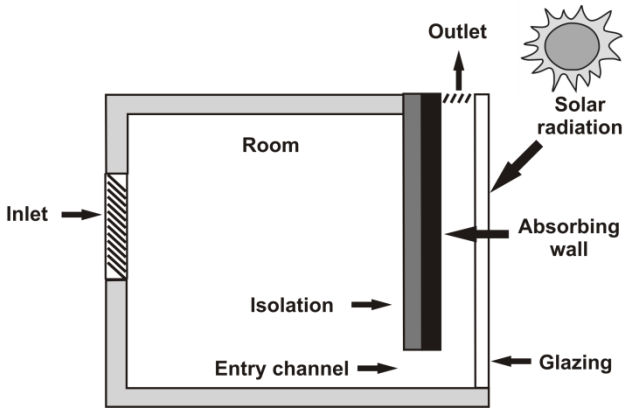

Fig. 2. Sketch of a solar chimney for building ventilation.

1.2. Literature review

Solar chimneys were developed in the 70s to obtain electric energy. The first practical application of a solar chimney was a pilot power plant built in Manzanares, near Madrid, Spain. The plant operated from 1982 to 1989 and generated approximately 50 kW electrical power [2, 3]. In the 90s decade chimneys began to be considered as a natural ventilation system for buildings [4, 5] but, from the start, the practical application of solar chimneys has been ahead of the technical studies in this field. Normally, ventilation solar chimneys are built without adequate calculation and dimensioning tools.

About the existing experimental researches, some of them concentrate on the analysis of the influence of geometric variables (width of the channel, air entrance area and chimney height) and on the effect of intensity of solar radiation on the generated air flow [6-10]. Other authors have developed prototypes and used their measurements to validate analytical or mathematical models [11-14]. Recently, Tan and Wong [15] assessed the natural ventilation performance of a classroom with a solar chimney situated in a zero energy building by performing several experiments.

The analytical models developed are based in application of energy balances among different components, normally characterizing each of them by unique temperature. Their main objective is usually the calculation of the air flow which can be extracted by this system and its instantaneous efficiency, defined as the relation between the energy received by the fluid and the income of solar radiation energy [4, 10-12, 16, 17]. Those analyses have obtained formulations, more or less adjusted to reality, but usually only from one dimensional point of view, and they do not provide detailed knowledge of the process which takes place inside the chimney. There are also some studies addressing more complex phenomena, for example, Martí-Herrero and Heras-Celemín [18] have evolved a mathematical dynamic model to evaluate the energetic performance of a solar chimney with a thermal inertia. They bear in mind some more detailed mechanisms, as the transient two-dimensional conduction through the wall which receives the

radiation. From the application point of view, several authors [19, 20] have analysed the performance of different solar chimneys designs by means of an algorithm which may be implemented in the computational software EnergyPlus for building simulation. Al-Kayiem et al., [21] studied the influence of the chimney height and collector area on the performance of a roof top solar chimney using a mathematical model. The results demonstrated that the performance of the system was highly influenced by solar intensity and wind speed.

CFD models for solar chimneys started to develop, more or less, at the same time as the experimental and analytical approaches, and its use has increased lately. Khanal and Lei [22] highlighted that although experimental investigations of solar chimney have dominated the existing literature, numerical modelling of solar chimney using CFD techniques has attracted increasing attention. Furthermore, it could be said that the numerical models have usually been used to evaluate the performance of specific cases, mostly with simplified boundary conditions. For example, Gan and Riffat [23] evaluated a particular solar chimney combined with a heat exchanger for heat recovery. Rodrigues et al., [24] applied a CFD model assuming constant temperature on the walls of the channel. Afonso and Oliveira [25] compared a solar chimney and a conventional one, both built in a test cell. Dubovsky et al., [26] developed a CFD numerical simulation of a dimensionally small chimney with results, fairly close to the experimental data. Wei et al., [27] carried out -with CFD techniques- a parametric analysis of two connected solar chimneys integrated in a two-storey house in China. Amori and Mohammed [28] studied the thermal and fluid-dynamic behaviour of a solar chimney located in Iraq, both experimentally and with a two-dimensional transient CFD model. More recently, Khanal and Lei [29] have analysed the airflow behaviour due to natural convection in a solar chimney using scaling analysis and numerical simulation. Tan and Wong [30] studied the influence of ambient air speed and internal heat load on the performance of solar chimney situated in the tropic, using both experimental data and numerical simulations.

Exergy analysis turned up in the 70s with the general purpose of promoting a more efficient use of the available energy sources. Plenty of publications explain, in detail, the general principles and the methodology of exergetic analysis together with the several options to define exergetic efficiency [31-34]. However, those methods are not still extensively applied to buildings thermal conditioning. A revision of the papers published on this subject can be found in Torío et al., [35] and Wang and Li [36]. Among the mentioned works, some of them can be emphasized, for instance the comparative study of energetic and exergetic efficiency of the heating systems of two residential buildings by Yang et al., [37] and the work by Zmeureanu and Yu Wu [38] who highlight the significance of the exergy concept in energy analysis and apply it to several heating, ventilation and hot water systems in residential buildings. Torío et al., [35] have also applied this methodology to direct solar systems (thermal and photovoltaic modules). Another significant work is that by Wang and Li [36], who used exergy to compare the performance of two ventilation systems, one of them fully natural and the other helped by solar energy. With regard to the study of exergy in solar chimneys, which is the subject of this paper, Petela [39, 40] and recently, Maia et al., [41] have developed an energetic and exergetic analysis of a solar chimney power

plant. However, the purpose of these systems (analysed in aforementioned works) is to obtain electric energy, and the analysis cannot be directly applied to solar chimneys used for building ventilation.

1.3. Objectives

The objectives of this work are the development of a numerical model (including the validation of this model with experimental data), the analysis of thermal and fluid-dynamic behaviour of the air inside the solar chimney and the performance of an exergetic analysis in order to evaluate ventilation power and efficiency of the chimney, looking for strategies or, more precisely, an analysis methodology to improve the design. A general purpose computational fluid-dynamic (CFD) software -FLUENT- has been used, which is able to solve three-dimensional turbulent flows and includes mathematical methods to simulate solar radiation (without any simplification). Exergetic variables are derived from the thermal and fluid-dynamic data obtained inside the chimney domain.

2. Exergetic analysis

Exergy is defined as the maximum theoretical useful work obtainable as the system interacts to equilibrium with an idealized system called environment, heat transfer occurring with the environment only [33]. One of the main uses of the exergy concept is in the exergy balance of thermal systems. The advantage, compared with the traditional energy balance, is that this analysis provides information on the quality or grades of energy crossing the thermal system boundary and about internal losses.

This paper applies the characteristics of the exergy concept in association with building heating and cooling systems as they have been described by Shukuya and Hammache [34]. In the absence of nuclear, magnetic and surface tension effects, the total exergy of a system can be divided into four components: physical exergy, kinetic exergy, potential exergy, and chemical exergy. In this case, the last one has not been considered because of the absence of chemical reactions.

The sum of the physical, kinetic and potential exergies is referred as thermo-mechanical exergy [31] and may be split into thermal exergy (due to the difference of temperatures between system and environment) and mechanical exergy (due to differences in pressure, kinetic and potential energy). Also, for a given uniform flow, the thermo-mechanical exergy transfer rate can be expressed as the mass flow multiplied by the specific exergy:

$$\vec{E}x = \vec{E}x^{T} + \vec{E}x^{M} = \dot{m} \cdot e \quad \vec{E}x = \vec{E}x^{T} + \vec{E}x^{M} = \dot{m} \cdot e \qquad (1)$$

Following Shukuya and Hammache [34] the specific exergy of an ideal gas is:

$$e = \int_{T_0}^{T} c_p dT - T_0 \int_{T_0}^{T} \frac{c_p}{T} dT + T_0 \cdot R \cdot ln\frac{p}{p_0} + \frac{v^2}{2} + g \cdot (z - z_0) e = \int_{T_0}^{T} c_p dT - T_0 \int_{T_0}^{T} \frac{c_p}{T} dT + T_0 \cdot R \cdot ln\frac{p}{p_0} + \frac{v^2}{2} + g \cdot (z - z_0) \qquad (2)$$

T_0, p_0 and z_0 are the temperature, pressure and height of the environment, and must be selected coherently with the process analysed.

If c_p may be considered constant:

$$e = c_p \cdot (T - T_0) - [T_0 \cdot c_p \cdot ln\frac{T}{T_0} - T_0 \cdot R \cdot ln\frac{p}{p_0}] + \frac{v^2}{2} + g \cdot (z - z_0)$$

$$e = c_p \cdot (T - T_0) - [T_0 \cdot c_p \cdot ln\frac{T}{T_0} - T_0 \cdot R \cdot ln\frac{p}{p_0}] + \frac{v^2}{2} + g \cdot (z - z_0)$$ (3)

Then:

$$e^T = c_p \cdot (T - T_0) - T_0 \cdot c_p \cdot ln\frac{T}{T_0} e^T = c_p \cdot (T - T_0) - T_0 \cdot c_p \cdot ln\frac{T}{T_0} \quad (4)$$

$$e^M = T_0 \cdot R \cdot ln\frac{p}{p_0} + \frac{v^2}{2} + g \cdot (z - z_0) e^M = T_0 \cdot R \cdot ln\frac{p}{p_0} + \frac{v^2}{2} + g \cdot (z - z_0) \quad (5)$$

Respectively, this expresses the specific thermal and mechanical exergy of a perfect gas.

As far as exergy balance is concerned, the ventilation solar chimney may be approached in a similar way to a solar chimney power plant [40]. But, in this case, the power extracted by the turbine in the power plant is used to overcome the flow losses needed for the building ventilation.

In the exergy balance (Fig. 3), the exergy given to the process is the sum of the exergy at the entrance plus the exergy of solar radiation; the exergy given by the process is the sum of the exergy at the exit plus the exergy of ventilation and plus, the exergy destruction due to irreversibility and losses.

$$\dot{Ex}_1 + \dot{Ex}_G = \dot{Ex}_2 + \dot{W}_V + \dot{Ex}_D \dot{Ex}_1 + \dot{Ex}_G = \dot{Ex}_2 + \dot{W}_V + \dot{Ex}_D \quad (6)$$

For an ideal gas and the specific conditions of a ventilation chimney, the difference between inlet and outlet flow exergy may be written as:

$$\dot{Ex}_2 - \dot{Ex}_1 = \dot{m} \cdot \left[c_P \cdot (T_2 - T_1) - T_0 \cdot c_P \cdot ln\frac{T_2}{T_1} + \frac{v_2^2}{2}\right] \dot{Ex}_2 - \dot{Ex}_1 = \dot{m} \cdot \left[c_P \cdot (T_2 - T_1) - T_0 \cdot c_P \cdot ln\frac{T_2}{T_1} + \frac{v_2^2}{2}\right] \quad (7)$$

where the following assumptions have been taken into account: the inlet pressure is the same as the outlet pressure ($p_2 = p_1$), the inlet height is also the same as the outlet height ($z_2 = z_1$) and the inlet velocity (v_1) is negligible compared with the outlet velocity (v_2).

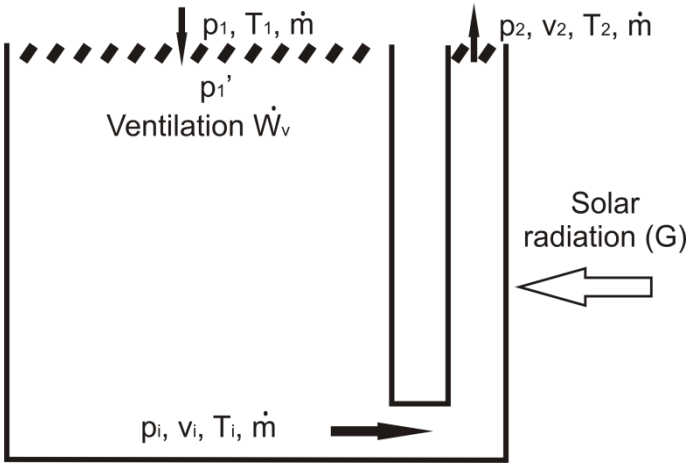

Fig. 3. Outline of the variables included in the analysis.

According to Petela [39], solar radiation exergy is

$$\dot{Ex}_G = \psi \cdot G \cdot b \cdot L \dot{Ex}_G = \psi \cdot G \cdot b \cdot L \quad (8)$$

$$\psi = 1 + \frac{1}{3} \cdot \left(\frac{T_0}{T_s}\right)^4 - \frac{4}{3} \cdot \frac{T_0}{T_s} \psi = 1 + \frac{1}{3} \cdot \left(\frac{T_0}{T_s}\right)^4 - \frac{4}{3} \cdot \frac{T_0}{T_s} \quad (9)$$

Where b and L are the width and length of the absorbing surface, G is the solar radiation and T_s is the solar radiation temperature.

The ventilation power is:

$$\dot{W_V} = \Delta p_v \cdot Q_1 \dot{W_V} = \Delta p_v \cdot Q_1 \quad (10)$$

$$\Delta p_v = p_1 - p_1' \Delta p_v = p_1 - p_1' \quad (11)$$

$$Q_1 = \frac{m}{\rho_1} = \dot{m} \cdot \frac{R \cdot T_1}{p_1} Q_1 = \frac{m}{\rho_1} = \dot{m} \cdot \frac{R \cdot T_1}{p_1} \quad (12)$$

To evaluate the efficiency of a steady state process, several exergy based relations may be used. Here, taking into account Bejan et al.´s definition [33], i.e. the ratio between the product (desired result produced by the system) and the fuel (the resources expended to generate the product), the total exergy efficiency would be:

$$\varphi = \frac{\dot{W_v} + (\dot{Ex_2} - \dot{Ex_1})}{\dot{Ex_G}} \varphi = \frac{\dot{W_v} + (\dot{Ex_2} - \dot{Ex_1})}{\dot{Ex_G}} \quad (13)$$

In the same way, the useful mechanical and thermal exergetic efficiency could be defined as

$$\varphi_u = \frac{\dot{W_v}}{\dot{Ex_G}} \varphi_u = \frac{\dot{W_v}}{\dot{Ex_G}} \quad (14)$$

$$\varphi_{mec} = \frac{\dot{W_v} + \dot{m} \cdot \frac{v_2^2}{2}}{\dot{Ex_G}} \varphi_{mec} = \frac{\dot{W_v} + \dot{m} \cdot \frac{v_2^2}{2}}{\dot{Ex_G}} \quad (15)$$

$$\varphi_{term} = \frac{\dot{m} \cdot c_P \cdot \left[(T_2 - T_0) - T_0 \cdot ln\frac{T_2}{T_0}\right]}{\dot{Ex_G}} \varphi_{term} = \frac{\dot{m} \cdot c_P \cdot \left[(T_2 - T_0) - T_0 \cdot ln\frac{T_2}{T_0}\right]}{\dot{Ex_G}} \quad (16)$$

These formulas are useful tools to understand the operation of a solar chimney, considered as a natural ventilation system. Specifically, the different types of exergetic efficiency allow the calculation of the performance of this building solution. However, the formulas do not enable to calculate temperature and mass flows, which should be obtained from experiments or from thermal and fluid dynamic models.

3. Methodology

In this paper the numerical simulation of the thermal and fluid-dynamic the solar chimney behaviour has been done with the Fluid Dynamic Computational Code FLUENT 6.3, which solves the Navier Stokes equations by the finite volumes method. The geometry of the three-dimensional model developed corresponds to the chimney studied by Ong and Chow [11]. Their results have been selected to validate the CFD model because their paper is one of the most detailed containing a lot of experimental data.

The inside chimney dimensions are 2 m height, 0.1 m air chamber thickness and 0.45 m width (Fig. 4). Because of symmetry, only half of the width is simulated; the front glass is 4 mm thick and the absorbing wall at the back is 22 mm thick. The entrance to the chimney channel is 0.1 m x 0.45 m. The room connected to the chimney is 1.78 x 2 x 0.45 m^3 with air inlet at its top.

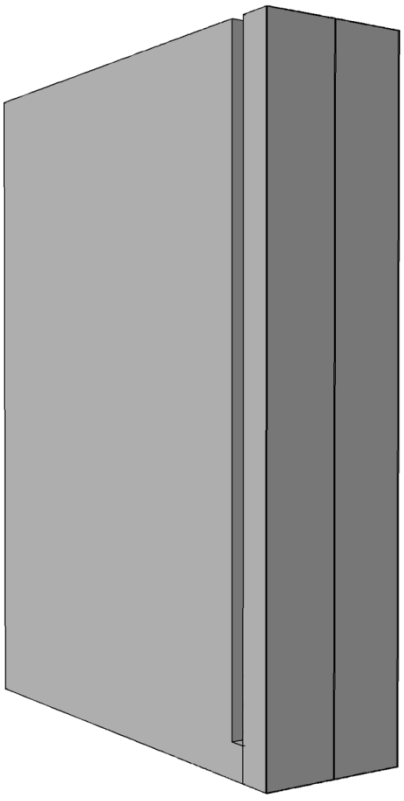

Fig. 4. Geometry of the solar chimney model.

A structured mesh with hexahedral elements has been developed, with an irregular distribution: refined in the channel, near the walls and where the flow could be more complex. Cell size progressively increases as the exit of the chimney is approached (Fig. 5). Meshes from 100,000 to 2 million cells were tested, founding non-significant differences in the results. The mesh of the final study has about 1 million cells, which allows a substantial spatial resolution.

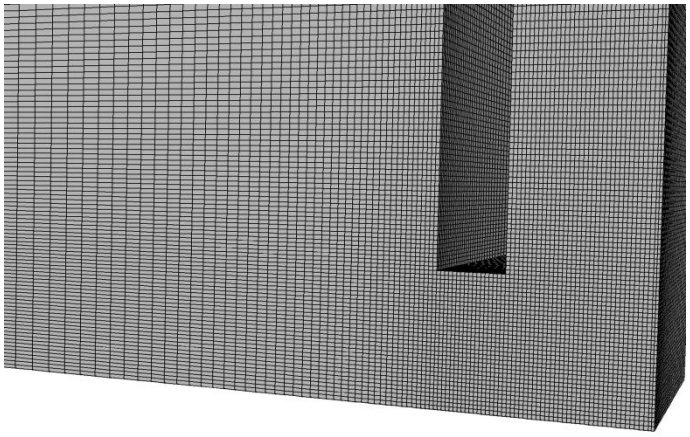

Fig. 5. Detail of the numerical model mesh.

The model solves the stationary viscous flow including the energy equation. For natural air convection, the Boussinesq approach has been taken; for turbulence, the K-epsilon (RNG) model and for solar radiation, the DO (Discrete Ordinates) model. The glass properties are 2220 kg/m^3 density, 830 J/kg·K heat at constant pressure, 1.03 W/m·K thermal conductivity, 1.52 refraction index, 0.84 external emission, 30 m^{-1}absorption coefficients in the visible band and 450 m^{-1} in the infrared band [42]. The opaque walls have the following properties: density 2800 kg/m^3, specific heat 856 J/kg·K, thermal conductivity 2.25 W/m·K and they are opaque with regard to solar radiation.

Air inlet is situated at the top of the room, and a condition of total pressure equal to the atmospheric pressure is imposed; the loss in this section is adjusted so that the same conditions as the aforementioned experimental model are obtained. The air exit is at the top of the chimney, with a constant static pressure boundary condition (also equal to the atmospheric pressure). The surfaces of the room are defined as adiabatic and so are the external surfaces of the absorbing walls. The external glass surface has boundary thermal condition allowing radiation and convection with the environment. The exterior temperature has been taken as 30ºC.

To analyse the fluid-dynamic and thermal behaviour of the solar chimney, simulations in steady state have been carried out, varying the solar radiation levels increasingly from 100 W/m^2 up to 700 W/m^2. These values correspond to the radiation at right angles with the glass exterior surface, as expressed by Ong and Chow [11], although the boundary condition has been applied with an inclination fitting the latitude of the experiment location.

As far as the resolution parameters are concerned, a second order discretization has been employed and, for the convergence, enough iterations to obtain normalized residues lower than10^{-5} were done.

4. Results

4.1. Validation

To validate the numerical CFD model, its results have been compared with the experimental data published by Ong and Chow [11]. Fig. 6a shows the comparison of mass flows and Fig. 6b the increase in temperature from the chimney inlet to its exit, both in function of solar radiation. These results indicate that the differences between the global behaviour of the numerical model and the experiment are smaller than 1.3%. Although it has not been plotted in the figures, the glass and the opaque walls temperature have differences lower than 2ºC. Therefore, the values of the variables inside the chimney calculated by the numerical model could be assumed as reasonably accurate.

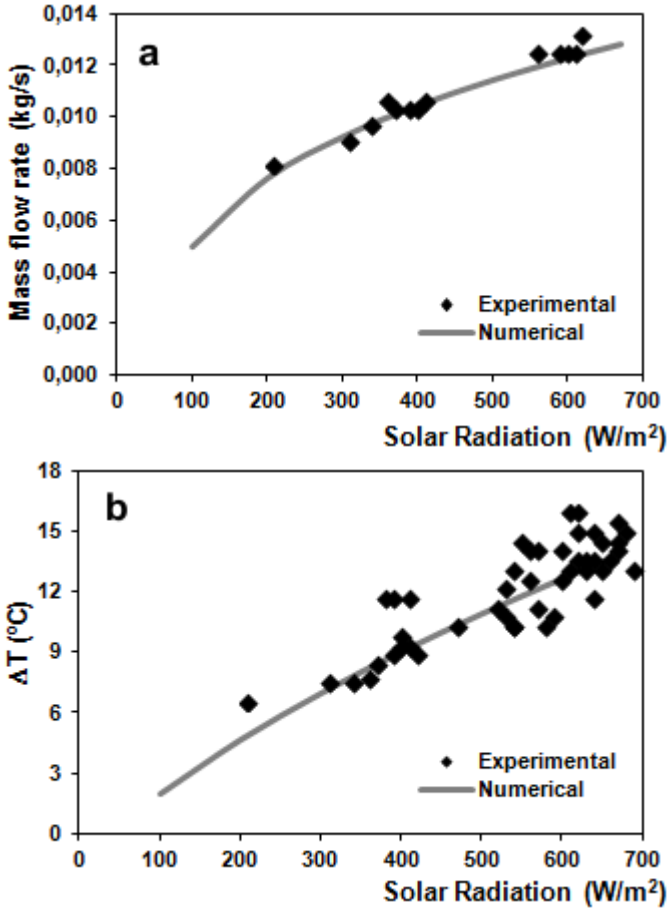

Fig. 6. Comparison between numerical and experimental values of the mass flow and the temperature increment in function of the solar radiation.

4.2. Qualitative analysis of thermal and fluid dynamic variables inside the chimney

To develop a deeper understanding of the phenomenon, firstly, an analysis of the thermal and fluid-dynamic variables is carried out with the results obtained in the numerical simulation. The case with a constant solar radiation of 300 W/m^2 has been selected for this analysis because it is an intermediate value of the available radiations.

Fig. 7 shows the temperature distribution of the surfaces and of air at the chimney vertical symmetry plane. The left figure has a bigger horizontal scale to give a better view of the chimney width. It can be seen that the absorbing surface gets the major part of the energy due to radiation; also, both this surface and the glass transfer the energy to the air flow, increasing its temperature as the air ascends inside the chimney. The distribution is asymmetric: higher in the absorbing wall and also, in the lateral opaque walls than in the glass. Due to the inclination of the sunbeam, the floor of the entrance channel of the chimney is partially heated, and a zone of higher temperature is therefore shown.

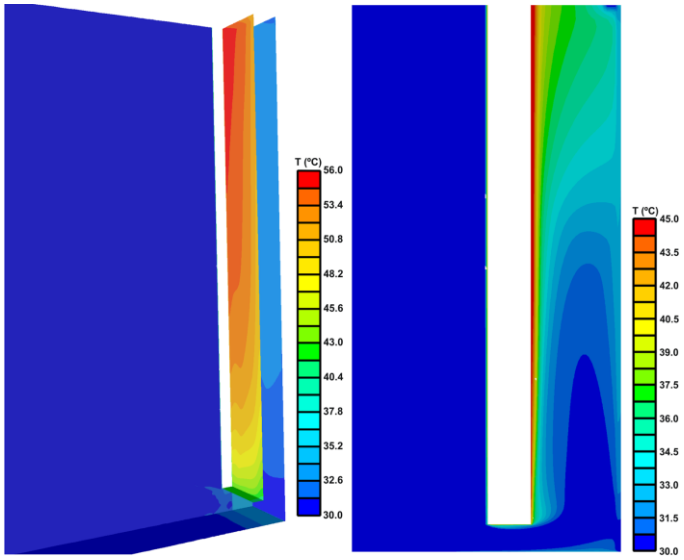

Fig. 7. Temperature distribution at the chimney surfaces (left). Air temperature distribution at the chimney symmetry plane (right). Solar radiation: 300 W/m^2, perpendicular to the glass surface.

In Fig. 8 the static pressure map at the left and the velocity magnitude at the right have been depicted, both in the symmetry plane. Pressure distribution is practically hydrostatic and slightly lower than the atmospheric pressure at the room entrance because of the loss at the inlet restriction. A slight difference of pressure distribution is appreciated between the chimney and the room, mainly in the lower pressure zones of inlet and outlet.

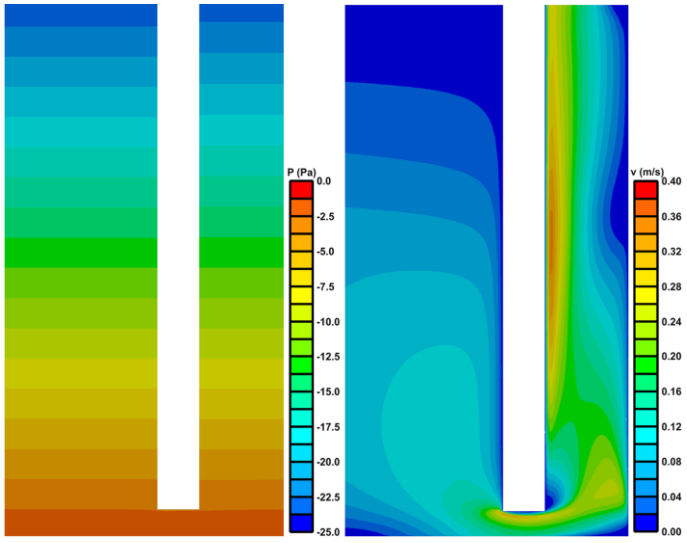

Fig. 8. Static pressure map in the chimney symmetry plane (left). Air velocity magnitude in the chimney symmetry plane (right). Solar radiation: 300 W/m^2, perpendicular to the glass surface.

Air velocity is clearly lower at room entrance and gradually, increases as it approaches the chimney channel. The stagnancy at the room floor before entering the chimney and at the lower part of the glass may also be noted. At the chimney entrance a high velocity zone is generated because of the sudden change in direction (higher velocity at the lower radius of curvature). Also, a flow separation is induced at the corner between the entrance and the channel. After that, the air flows towards the glass due to the inertia. In spite of this, in its ascending path the heat transfer to the air flow is higher near the absorbing wall opposed to the glass, therefore, increasing more its velocity in this side of the channel. The higher velocity is found at the medium height zone because, as the flow goes up, there is a heat transfer in the air towards the central part of the channel, which tends to reduce the velocity and temperature differences across the channel. The maximum value of the velocity is quite low, around 4 m/s. However, measuring ventilation in renewals per hour as it is usual, the ventilation flow is on the range of 25 m^3/hour, enough for a medium-sized room.

The air flow in the entrance to the chimney channel may be seen in detail in Fig. 9 with stream lines coloured with the velocity magnitude. In this figure, the flow separation at the corners of the entrance is clearly shown. Although kinetic energy has small influence in the energy balance, the flow detail has a greater importance, particularly for the heat transfer in the more complex zones. For instance, the separation could be diminished as well as the pressure losses by rounding off the corners at the entrance. The drawback is that this will also reduce turbulence and therefore, the heat transfer. Furthermore, the flow would be closer to the absorbing surface in its lower part, which would improve energy transfer in that zone.

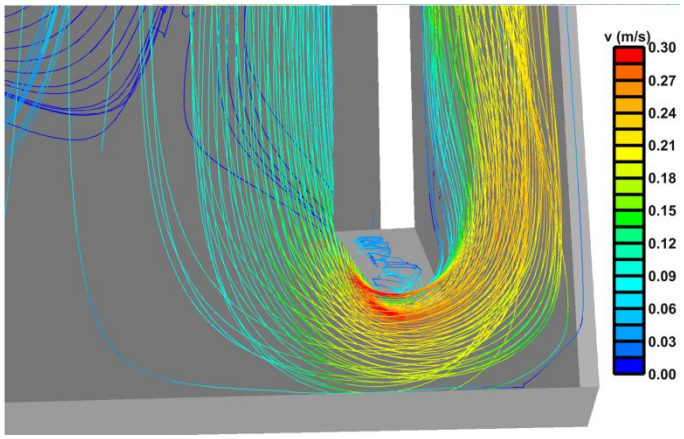

Fig. 9. Streamlines of air flow at the entrance of the chimney channel; coloured by velocity magnitude (300 W/m^2 solar radiation, perpendicular to the glass surface).

Specific exergy, both mechanical and thermal, have been calculated and may be seen in Fig. 10, also for the vertical symmetry plane and solar radiation of 300 W/m^2. Environment values are T_0=30ºC, p_0=101300 Pa and z_0 = 0 (reference or dead state values). The variation of mechanical exergy is dominated by the pressure; in the adjacent room this term increases as the air approaches the chimney entrance even if there is a decrease in potential exergy. In the chimney channel the process is reverse. In this last zone, the kinetic exergy influence can be noted as, transversally, the specific mechanical exergy is larger where the velocity magnitude is higher, that is, near the glass at the bottom part and near the absorbing surface at the middle and top. Referring to thermal exergy, in the adjacent room no variation is noticed; along the chimney height it slowly increases near the absorbing surface. From the beginning of the last third of the height the increase in thermal exergy is extended through the whole channel, with an asymmetric profile because the absorbing surface has a bigger temperature than the glass; the effect is more obvious in exergy than in temperature. Thermal exergy values are much bigger than those of the mechanical exergy. In fact, the thermal values are one order of magnitude larger and its variation still greater. It can, therefore, be said that total exergy basically coincide with thermal exergy.

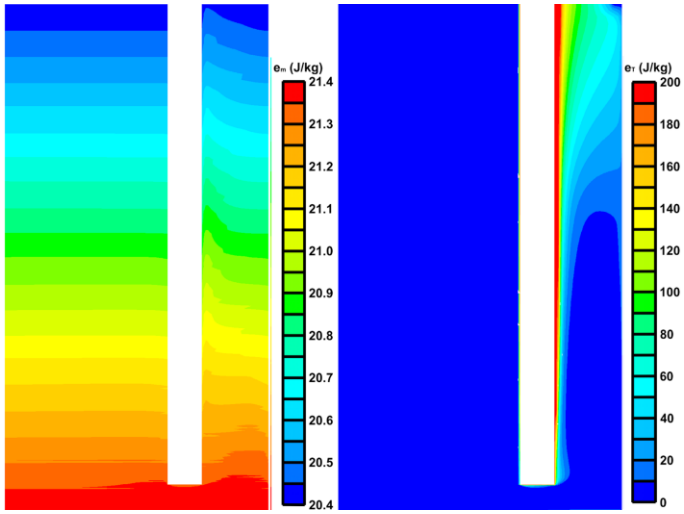

Fig. 10. Specific mechanical exergy (left) and specific thermal exergy (right), both in the chimney symmetry plane (300 W/m^2 solar radiation, perpendicular to the glass surface).

4.3. Quantitative analysis of thermal and fluid dynamic variables inside the chimney

To observe the evolution of variables inside the chimney and to show their values in a more quantitative form, three flow (or path) lines have been selected and shown in Fig. 11 and 12. They have been drawn at the symmetry plane, with a solar radiation of 300 W/m^2 perpendicular to the glass surface; pl 2 corresponds to the intermediate mass flow and pl 1 and 3 to 95% and 5% respectively. Three characteristics may be emphasized about the spatial distribution of the flow lines. Firstly, the stagnancy zone in the lower right corner of the room, which is due to the position of the entrance at the ceiling; anyhow, as it will be seen, the values in the room have almost no variations and the flow distribution in it do not affect the performance of the chimney. Secondly, the sharp turn at chimney entrance: the inner line, pl 3, shows the flow detachment from the corner; pl 2 shifts towards the inner side because of the irrotational tendency of the flow outside the losses zone; velocity increases with the radius of curvature diminution. Further on the line separates a little from the wall because of inertia. Thirdly, the gradual shift toward the absorbing wall: in the lower part, the inner line (pl 3), just after the curve; then the middle line (pl 2), from around 1/3 of the height; last the outer line (pl 1) from half of the height. This concentration of the lines shows a higher mass flow near the absorbing wall, due to higher temperatures and consequent bigger velocities in its proximity.

Fig. 11a shows the temperature distribution along the three flow lines. In this and following figures the length of the trajectory has been displaced to get position 0 at the channel entrance, the way through the room with negative coordinates and the ascension inside the chimney with positive values. This shift does not affect the analysis and allows a clearer view of the phenomenon. Temperatures in the adjacent room remain at the same value of the air entrance. The flow line nearer the floor (pl 1) begins to heat even before the channel entrance because the floor is heated by the incidence of the sloped solar beams. The channel presents a large temperature difference between the line nearest the absorbing surface and the other two. Along this flow line (pl 3), the temperature increase is much higher in the lower half of the chimney than in the upper part. This is due to the reduction of convection heat transfer from the wall as the air gets hotter, and the width of the thermal boundary layer increases.

Velocities along the three flow lines (Fig. 11b) show a progressive increase in the room as they get closer to the chimney entrance. The entrance and the turn at the beginning of the chimney is a complex zone due to the inertia, detachment and stagnancy phenomena. From the height of 0.2-0.3 m to the middle height of the channel (1.1-1.2 m) the mass flow concentrates towards the absorbing surface, increasing the velocities of lines pl 2 and pl 3, and decreasing at the same time that of pl 1. From middle height up the distribution has a certain tendency to steady down with an increase in pl 1 velocity and decrease of pl 2 and 3, although those last two remain clearly higher.

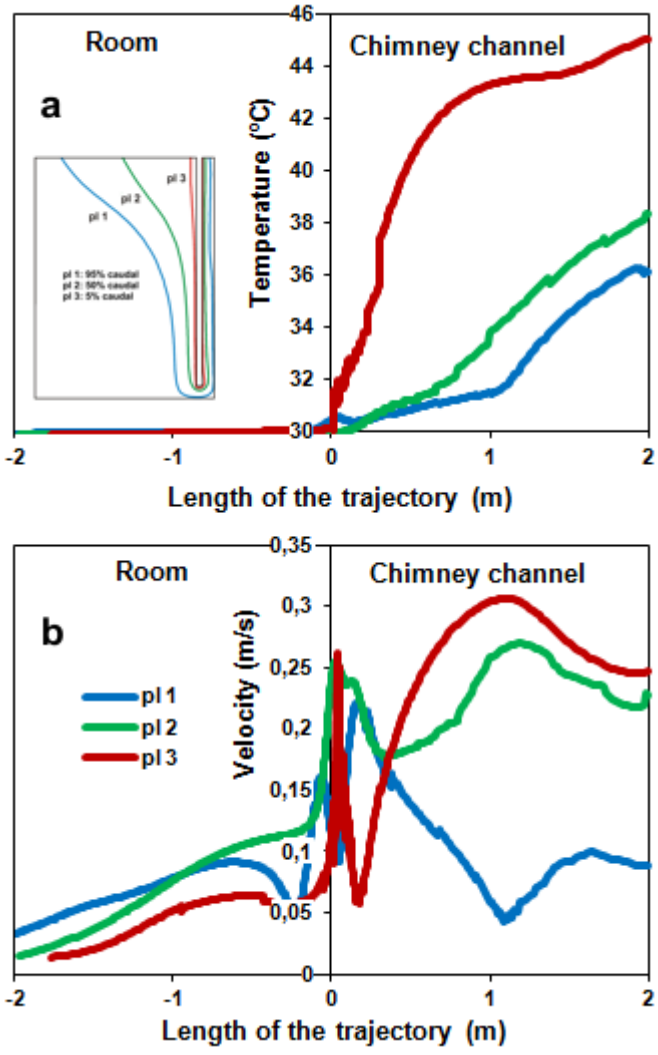

Fig. 11. Evolution of the temperature (a) and the velocity magnitude (b) along the three flow lines.

Fig. 12a shows the changes in the specific thermal exergy. Basically, the trends are very similar to those of the temperature, although the difference between the inner flow line (pl 3) and the other two is bigger and the slope of this inner line is higher in the top quarter of the chimney. The middle line (pl 2) does not start gaining exergy up to 0.5 m and the outer line (pl 1) up to 1 m. The mechanical specific exergy is represented in Fig. 12b. As it has been previously commented, it increases when the air descends towards the channel entrance and decreases upwards the chimney. The apparent difference amongst the three lines in the adjacent room is due to the mentioned coordinate positioning. In fact, as was shown in Fig. 12b, the three values referred to the same height are practically equal, with fewer differences in the adjacent room than in the chimney channel. The flow line pl 3 has a slightly lower specific exergy at the beginning of the channel, perhaps due to the lower velocity and the pressure loss at the corner. From 0.5 m up it is a little bigger than the other two because of the higher air velocity near the absorbing surface.

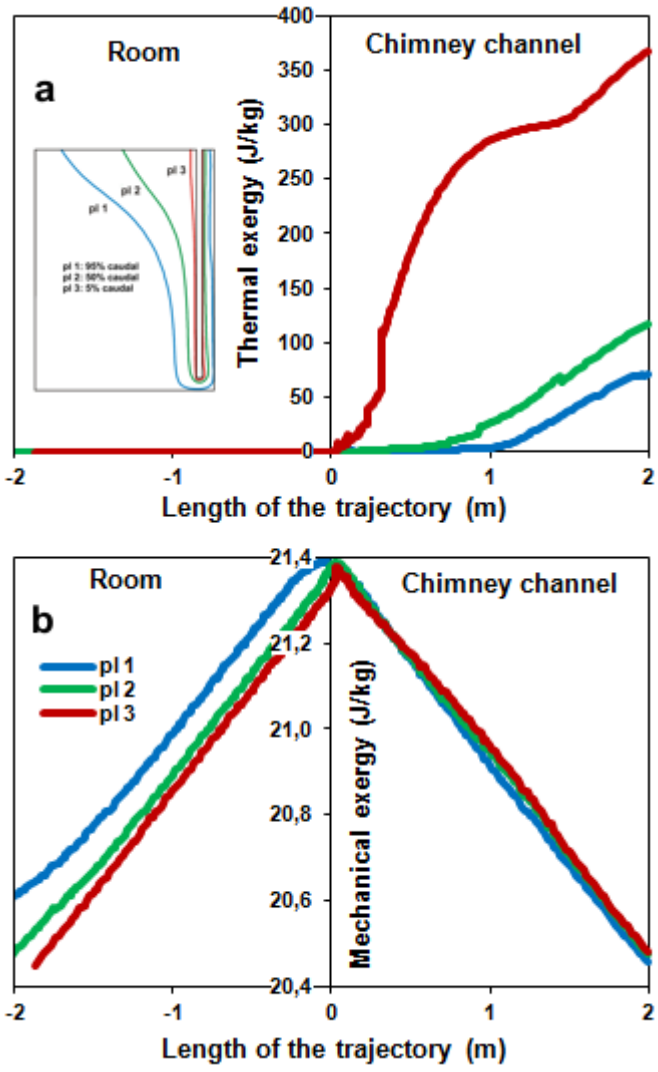

Fig. 12. Evolution of the specific thermal (a) and mechanical (b) exergy along the three flow lines.

4.4. Quantitative analysis of thermal and fluid dynamic variables at chimney exit

The exergy balance at the exit has to be established by integration on the exit area because neither the specific exergies nor the mass flow is uniform in that section. To assess this lack of uniformity, an analysis of the values of different variables at the exit section will be carried out in the following paragraphs.

In Fig. 13, the horizontal coordinate is a horizontal line in the symmetry plane, from the absorbing wall (0 m) to the glass (0.1 m). Velocity and temperature distributions are shown in Fig. 13a. Velocity values are zero at the glass and the wall, consistently with the non-slip condition of the flow. From 0.085 to 0.1 m, velocity takes negative values due to a small recirculation loop at the exit section, which is sometimes found in solar chimneys [21]. Apart from that, the velocity profile is basically linear (triangular profile) between glass and wall. The recirculation loop may also be observed in the temperature distribution, where the value is equal to that

in the surrounding space. Near the wall, the temperature decreases strongly in the first 10% of the width, showing the thermal boundary layer. The specific exergies, thermal and mechanical can be seen in Fig. 13b. Both have their lower values in the recirculation loop. Concerning mechanical exergy, pressure and height values being constant in this section, the tendency follows that of the square of velocity, i.e. the variation is that of the kinetic energy. The thermal exergy has a trend which is very similar to that of the temperature. It has a sharper increase inside the thermal boundary layer, because the energy quality is higher when the temperature increases. To obtain the outlet flow exergy, the specific exergy has to be integrated with the differential of mass flow, that is the surface integral of specific exergy multiplied by the density and by the velocity component at square angles to the exit area. Those values, mechanical and thermal, have been represented in Fig. 13c as exergy flow per unit area. Their values show similar tendencies to those of the previous figure. However, the mechanical flow exergy is somewhat higher in the central zone than closer to the wall because the mass flow is lower due to higher temperatures near the wall, and the thermal flow exergy falls to zero at the wall (the same as velocity). The integration gives an exit mechanical flow exergy of 0.207 W and exit thermal flow exergy of 1.404 W. If the temperature and velocity values were uniform (doing the calculations with the mean values), the mechanical flow exergy obtained would be only 0.07% lower whereas the thermal flow exergy would be 6.7% lower. The variation between the wall and the glass increases the exit flow exergy with respect to the value that could be obtained if the temperature and velocity where more homogeneous. This, in turn, means a reduction of the ventilation power achievable. In any case, this is one of the reasons why CFD numerical models can be far more accurate than analytical models, which assume uniform temperature and velocity distribution.

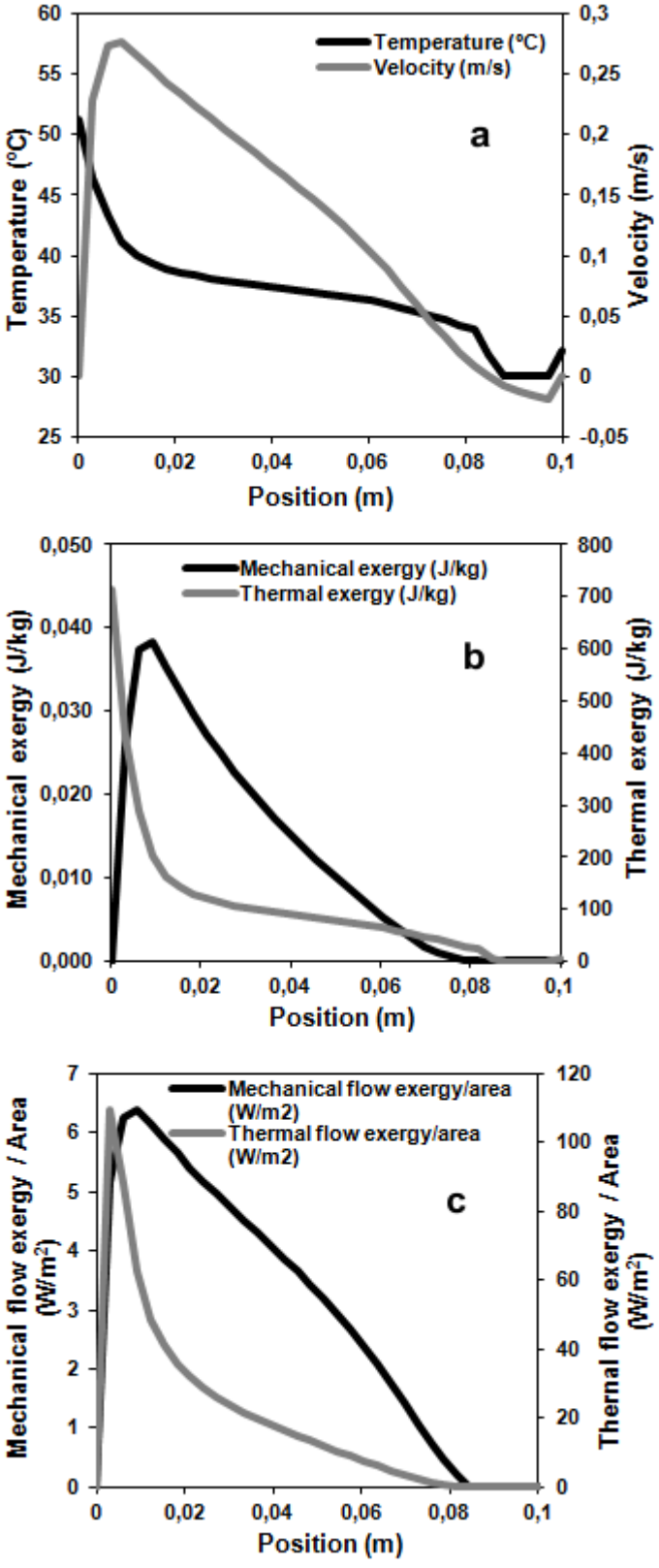

Fig. 13. a. Air temperature and velocity at the exit of the solar chimney over the symmetry plane, from the absorbing wall (left axis) to the glass (right).
b. Specific thermal and mechanical exergy at the exit of the solar chimney over the symmetry plane.
c. Mechanical and thermal flow exergy per unit area at the exit of the solar chimney over the symmetry plane.
Solar radiation: 300 W/m^2, perpendicular to the glass surface.

4.5. Exergetic efficiencies and global analysis

From an overall point of view, formulas 13 to 16 enable us to obtain the values of the useful, mechanical, thermal and total efficiency that are represented in Fig. 14. The difference between the useful and the mechanical exergy is only the kinetic energy at the exit. It may be noted that this term is not negligible (about 10%), which suggests that a reduction of the exit velocity (perhaps with a wider outlet) would be advisable. Another feature of these efficiencies is that its slope is reduced when radiation increases; it decreases even more than the trend found in the mass flow (Fig. 6a). This is coherent with higher pressure losses due to the flow separation and friction (which are expected to increase with the square of velocity). This losses can be reduced rounding the corners and with a lower and more uniform transversal velocity distribution. Lower velocity could be achieved increasing the channel depth, but this has the drawback of increasing the non-uniformities and other phenomena as the outlet recirculation. A careful study of the channel geometry has to be made to optimize these conflicting effects. Thermal and total exergetic efficiencies are practically equal and one order of magnitude greater than the mechanical; also, the slope is quite steady with increasing radiation. From a more quantitative point of view, the values of the case taken as representative, corresponding to a solar radiation of 300 W/m^2 (perpendicular to the glass surface) are the following: solar flow exergy: 251.82 W, difference between inlet an exit flow exergy: 1.4047 W, ventilation power: 0.0016 W. According to equation 6, the exergy losses are 250.41 W then. The useful exergetic efficiency is 0.0006%, and the thermal exergetic efficiency is 0.55%; these values are quite low but, as the fuel (solar radiation) is cheap, this inconvenient is not a major one. However, their relative values indicate that this construction could be more appropriate as a heating device than as a ventilation one.

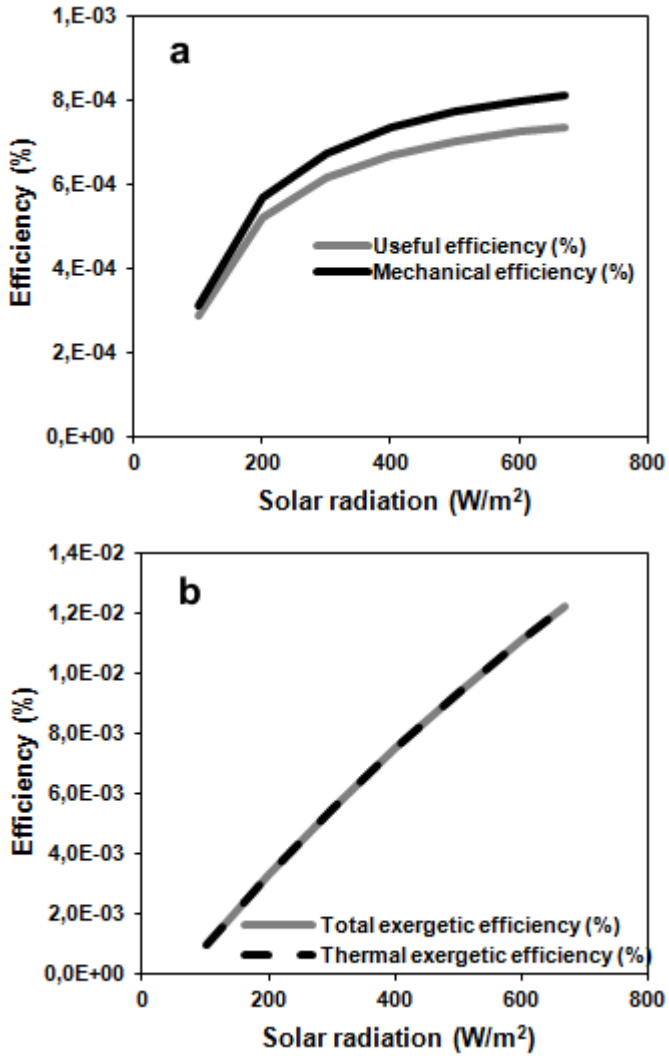

Fig. 14. Useful and mechanical efficiency (a), thermal and total exergetic efficiency (b) in function of the solar radiation.

The specific thermal exergy could be increased if the flow temperatures were higher, though this should not be attained lowering the mass flow because the exergy flow will decrease accordingly. On the one hand, the mass flow is intrinsically related to the channel temperatures: a higher temperature of the channel air flow would mean lower densities and higher pressure differences which will, in turn, produce larger mass flows. On the other hand, the solar energy rate is 270 W and the difference between inlet and outlet energy rate is about 90 W. As the walls are heavily isolated, the comparison of the last two values indicates that 2/3 of the incoming solar power is lost at or through the glass (reflection, convective and radiative losses to the exterior). The reduction of these losses could be the most effective way to enhance the chimney performance and efficiency. However, this is a difficult task because reducing the losses through the glass (with a thicker or double glass, for example) will also restrict the incoming solar radiation. Again, an optimization analysis has to be made to maximize the final result.

A global economic study has not been considered worthwhile as the ventilation power obtained is in the order of milliwatts.

5. Conclusions

This paper begins with a general exergetic analysis applied to solar chimneys used for building ventilation, defining the specific exergies, its balances and efficiencies. Afterwards, a CFD three-dimensional model has been generated to analyse the thermal and dynamic behaviour of the fluid in a solar chimney. The results were validated with data available in the bibliography, obtaining a good correspondence. From the numerical results, both a qualitative and a quantitative analysis of the thermal and fluid-dynamic variables inside and at the exit section of the chimney were performed.

About the temperature distribution, the results show a larger increase of the temperature of the ascending air near the absorbing opaque wall than at the glass side. The velocity maps reflect the complex flow pattern, mainly at the channel entrance. The mean velocity values are quite low but enough flow is generated to ventilate a room.

The thermal and mechanical exergy distributions were estimated inside the chimney, noticing that the mechanical one is governed by the pressure term. The thermal exergy increases going up in the chimney, following the temperature tendencies. Besides, the thermal exergy is always fairly greater than the mechanical one. The previous variables have been quantitatively analysed along three path lines and, also, at the chimney exit. Those analyses have allowed us to determine the most problematic points for its performance: the separation in the turn at the channel entrance, the recirculation loop at the exit section, the lack of uniformity of temperature and velocity distributions for different chimney sections, etc. Finally, the exergetic efficiencies were calculated and a global analysis preformed.

This study suggests that the crucial points to improve the chimney performance are the minimization of the fluid dynamic losses, the optimization of the channel geometry with respect to the transversal variables distribution and the reduction of the losses through the glass while maintaining the incoming radiation. To improve the chimney design, it will be necessary to perform an extensive parametric study on the effects of the chimney geometry.

From the economic point of view, although fuel is cheap, the financial costs of the investment are not. As the ventilation power achieved is in the order of milliwatts, the reasons for the use of solar chimneys in building ventilation will remain within the sphere of architectural decisions.

6. Acknowledgements

This work was carried out in the framework of the Singular Strategic Project ARFRISOL, on bioclimatic architecture and solar cooling (Reference: PS-120000-2005-1), funded by the Spanish Ministry of Education and Science (MEC) and co-funded by ERDF.

7. References

[1] International Energy Agency (IEA), Worldwide trends in energy use and efficiency. Key insights form IEA Indicator Analysis. Head of Communication and Information Office, Paris, France, 2008. http://www.iea.org/Textbase/about/copyright.asp.

[2] W. Haaf, K. Friedrich, G. Mayr, J. Schlaich, Solar chimneys, Part I: Principle and construction of the pilot plant in Manzanares, International Journal of Sustainable Energy 2 (1983) 3-20.

[3] W. Haaf, Solar chimneys, Part II: Preliminary test results from the Manzanares pilot plant, International Journal of Sustainable Energy 2 (1984) 141-161.

[4] N.K. Bansal, R. Mathur, M.S. Bhandari, Solar chimney for enhanced stack ventilation, Building and Environment 28 (1993) 373-377.

[5] H.B. Awbi, Design considerations for naturally ventilated buildings, Renewable Energy 5 (2) (1994) 1081-1090.

[6] A. Bouchair, Solar chimney for promoting cooling ventilation in Southern Algeria, Building Services Engineering Research & Technology 15 (2) (1994) 81-93.

[7] M.J. Swainson, Evaluation of the potential of solar chimneys to drive natural ventilation in non-domestic buildings. Ph.D. Thesis, Cranfield University, UK, 1997.

[8] J. Hirunlabh, W. Kongduang, P. Namprakai, J. Khedari, Study of natural ventilation of houses by a metallic solar wall under tropical climate, Renewable Energy 7 (1999) 109-119.

[9] S. Spencer, An experimental investigation of a solar chimney ventilation system. Ph.D. Thesis in the Department of Building, Civil and Environmental Engineering, Concordia University, Canada, 2001.

[10] Z.D. Chen, P. Bandopadhayay, J. Halldorsson, C. Byrjalsen, P. Heiselberg, Y. Li, An experimental investigation of a solar chimney model with uniform wall heat flux, Building and Environment 38 (2003) 893-906.

[11] K.S. Ong, C.C. Chow, Performance of solar chimney, Solar Energy 74 (2003) 1-17.

[12] N.K. Bansal, J. Mathur, S. Mathur, M. Jain, 2005. Modeling of window-sized solar chimneys for ventilation, Building and Environment 40 (2005) 1302-1308.

[13] J. Martí, Caracterización de una chimenea solar a través de parámetros físicos como sistema de ventilación natural. Tesis Doctoral, Departamento de Física de los Materiales, Facultad de Ciencias, Universidad Nacional de Educación a Distancia, 2006.

[14] J. Arce, M.J. Jiménez, J.D. Guzmán, M.R. Heras, G. Álvarez, J. Xamán, Experimental study for natural ventilation on a solar chimney, Renewable Energy 34 (2009) 2928-2934.

[15] A.Y.K. Tan, N.H. Wong, Natural ventilation performance of classroom with solar chimney system, Energy and Buildings 53 (2012) 19-27.

[16] Z. Adam, T. Yamanaka, H. Kotani, Mathematical model and experimental study of airflow in solar chimneys, in: Proceedings of 8th International Conference on Air Distribution in Rooms (ROOMVENT 2002).

[17] K.S. Ong, A mathematical model of a solar chimney, Renewable Energy 28 (2003) 1047-1060.

[18] J. Martí-Herrero, M.R. Heras-Celemín, 2007, Dynamic physical model for a solar chimney, Solar Energy 81 (2007) 614-622.

[19] K.H. Lee, R.K. Strand, Enhancement of natural ventilation in buildings using a thermal chimney, Energy and Buildings 41 (2009) 615-621.

[20] X. Jianliu, L. Weihua, Study on solar chimney used for room natural ventilation in Nanjing, Energy and Buildings 66 (2013) 467-469.

[21] H.H. Al-Kayiem, K.V. Sreejaya, S.I. Ul-Haq Gilani, Mathematical analysis of the influence of the chimney height and collector area on the performance of a roof top solar chimney, Energy and Buildings 68 (2014) 305-311.

[22] R. Khanal, C. Lei, Solar chimney – A passive strategy for natural ventilation, Energy Buildings 43 (2011) 1811-1819.

[23] G. Gan, S.B. Riffat, A numerical study of solar chimney for natural ventilation of buildings with heat recovery, Applied Thermal Engineering 18 (1998) 1171-1187.

[24] A.M. Rodrigues, A. Canha, A. Lahellec, J.Y. Grandpeix, Modelling natural convection in a heated vertical channel for room ventilation, Building and Environment 35 (2000) 455-469.

[25] C. Afonso, A. Oliveira, Solar chimneys: Simulation and experiment, Energy and Buildings 32 (2000) 71-79.

[26] V. Dubovsky, G. Ziskind, S. Druckman, E. Moshka, Y. Weiss, R. Letan, Natural convection inside ventilated enclosure heated by downward-facing plate: experiments and numerical simulations, International Journal of Heat and Mass Transfer 44 (16) (2001) 3155-3168.

[27] D. Wei, Y. Qirong, Z. Jincui, A study of the ventilation performance of a series of connected solar chimneys integrated with building, Renewable Energy 36 (2011) 265-271.

[28] K.E. Amori, S.W. Mohammed, Experimental and numerical studies of solar chimney for natural ventilation in Iraq, Energy and Buildings 47 (2012) 450-457.

[29] R. Khanal, C. Lei, A scaling investigation of the laminar convective flow in a solar chimney for natural ventilation, International Journal of Heat and Fluid Flow 45 (2014) 98-108.

[30] A.Y.K. Tan, N.H. Wong, Influences of ambient air speed and internal heat load on the performance of solar chimney in the tropics, Solar Energy 102 (2014) 116-125.

[31] M.J. Moran, Availability analysis: A guide to efficient energy use. Prentice Hall, Englewood Cliffs, NJ, 1982.

[32] R.A. Gaggioli, Available energy and exergy, International Journal of Applied Thermodynamics 1 (1-4) (1998) 1-8.

[33] A. Bejan, G. Tsatsaronis, M. Moran, Thermal design and optimization. John Wiley & Sons, New York, USA, 1996.

[34] M. Shukuya, A. Hammache, Introduction to the concept of exergy – For a better understanding of low-temperature-heating and high-temperature-cooling systems, in: VTT research notes 2158, Espoo, Finland, 2002.

[35] H. Torío, A. Angelotti, D. Schmidt, Exergy analysis of renewable energy-based climatisation systems for buildings: A critical view, Energy and Buildings 41 (2009) 248-271.

[36] L. Wang, N. Li, Evaluation of buoyancy-driven ventilation in respect of exergy utilization, Energy and Buildings 42 (2010) 221-229.

[37] L. Yang, R. Zmeureanu, H. Rivard, Comparison of environmental impacts of two residential heating systems, Building and Environment 43 (6) (2008) 1072-1081.

[38] R. Zmeureanu, X. Yu Wu, Energy and exergy performance of residential heating systems with separate mechanical ventilation, Energy 32 (3) (2007) 187-195.

[39] R. Petela, Exergy of undiluted thermal radiation, Solar Energy 74 (2003) 469-488.

[40] R. Petela, Thermodynamic study of a simplified model of the solar chimney power plant, Solar Energy 83 (2009) 94-107.

[41] C.B. Maia, J.O. Castro Silva, L. Cabezas-Gómez, S.M. Hanriot, A.G. Ferreira, Energy and exergy analysis of the airflow inside a solar chimney, Renewable and Sustainable Energy Reviews 27 (2013) 350-361

[42] V.P. Nicolau, F.P. Maluf, F.P., Determination of radiative properties of commercial glass, in: Proceedings of PLEA2001 Conference on Passive and Low Energy Architecture, Florinápolis, Brazil, 2001.

Figure captions.

Fig. 1: CIEMAT research building at Almería's Solar Platform. Solar chimney detail.

Fig. 2: Sketch of a solar chimney for building ventilation.

Fig. 3: Outline of the variables included in the analysis.

Fig. 4: Geometry of the solar chimney model.

Fig. 5: Detail of the numerical model mesh.

Fig. 6: Comparison between numerical and experimental values of the mass flow and the temperature increment in function of the solar radiation.

Fig. 7: Temperature distribution at the chimney surfaces (left). Air temperature distribution at the chimney symmetry plane (right). Solar radiation: 300 W/m2, perpendicular to the glass surface.

Fig. 8: Static pressure map in the chimney symmetry plane (left). Air velocity magnitude in the chimney symmetry plane (right). Solar radiation: 300 W/m2, perpendicular to the glass surface.

Fig. 9: Streamlines of air flow at the entrance of the chimney channel; coloured by velocity magnitude (300 W/m^2 solar radiation, perpendicular to the glass surface).

Fig. 10: Specific mechanical exergy (left) and specific thermal exergy (right), both in the chimney symmetry plane (300 W/m^2 solar radiation, perpendicular to the glass surface).

Fig. 11: Evolution of the temperature (a) and the velocity magnitude (b) along the three flow lines.

Fig. 12: Evolution of the specific thermal (a) and mechanical (b) exergy along the three flow lines.

Fig. 13: a. Air temperature and velocity at the exit of the solar chimney over the symmetry plane, from the absorbing wall (left axis) to the glass (right). b. Specific thermal and mechanical exergy at the exit of the solar chimney over the symmetry plane. c. Mechanical and thermal flow exergy per unit area at the exit of the solar chimney over the symmetry plane. Solar radiation: 300 W/m2, perpendicular to the glass surface.

Fig. 14: Useful and mechanical efficiency (a), thermal and total exergetic efficiency (b) in function of the solar radiation.

Figure(s)

Click here to download high resolution image

Figure(s)
Click here to download high resolution image

Figure(s)
Click here to download high resolution image

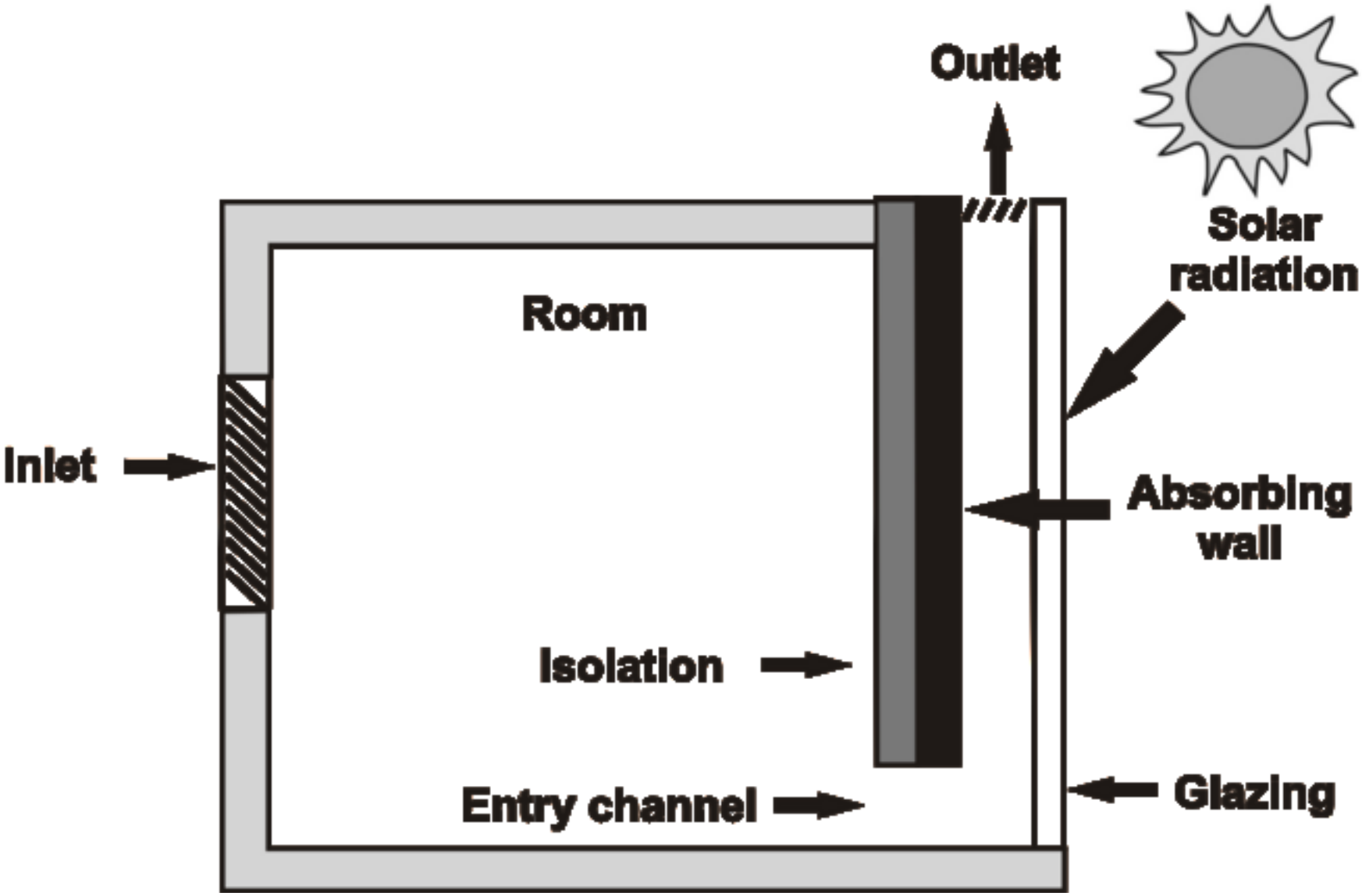

Figure(s)
Click here to download high resolution image

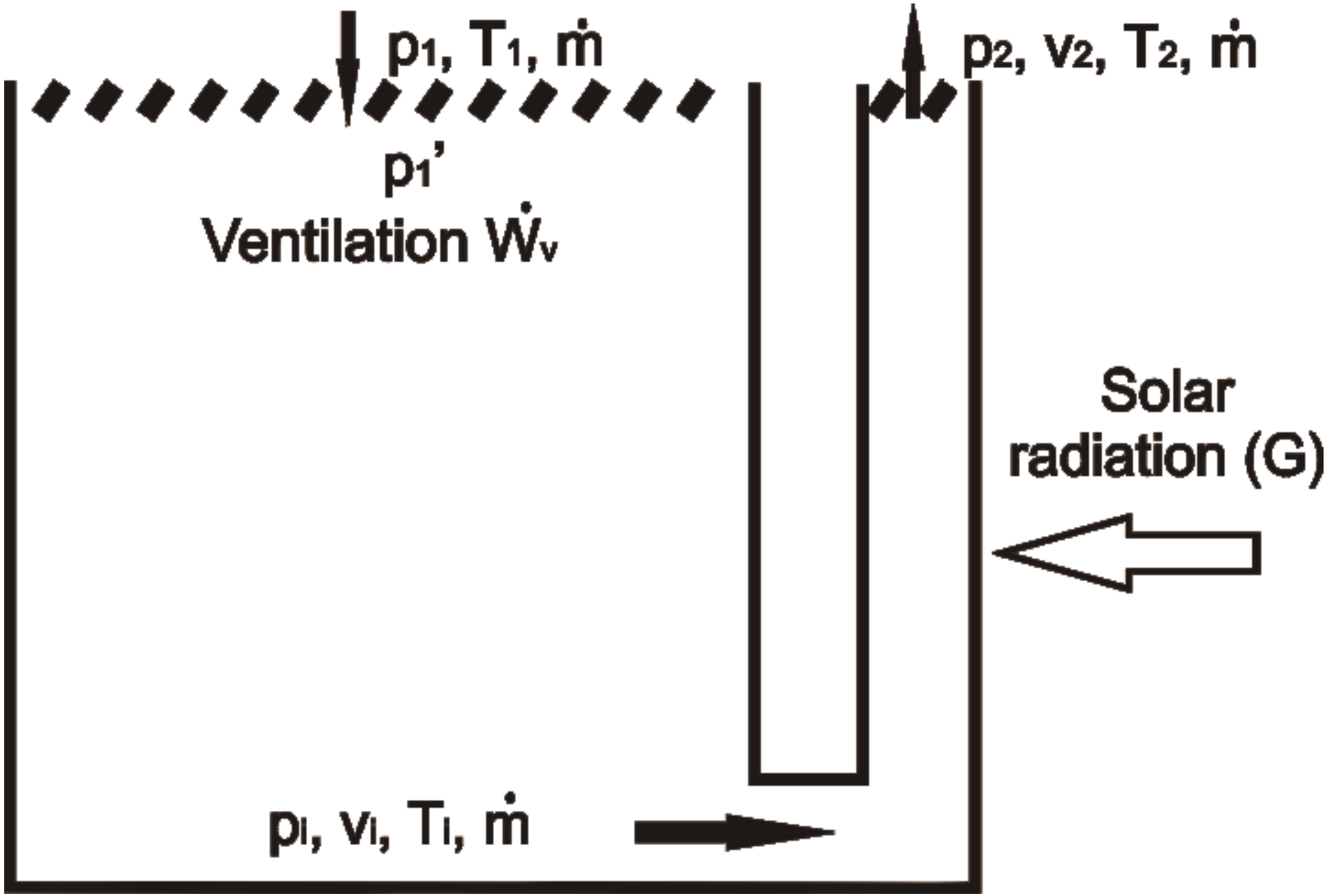

Figure(s)

Click here to download high resolution image

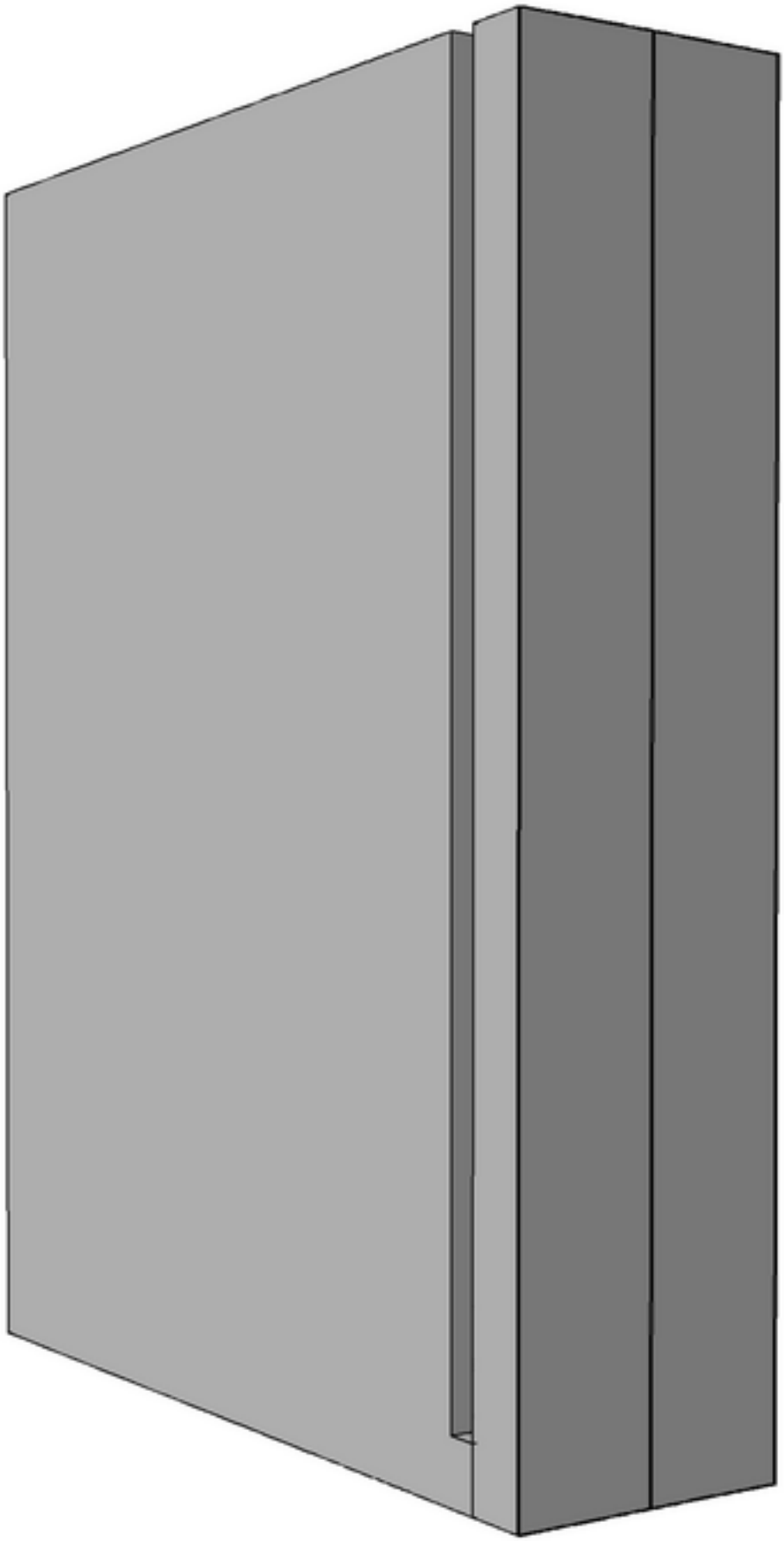

Figure(s)

Click here to download high resolution image

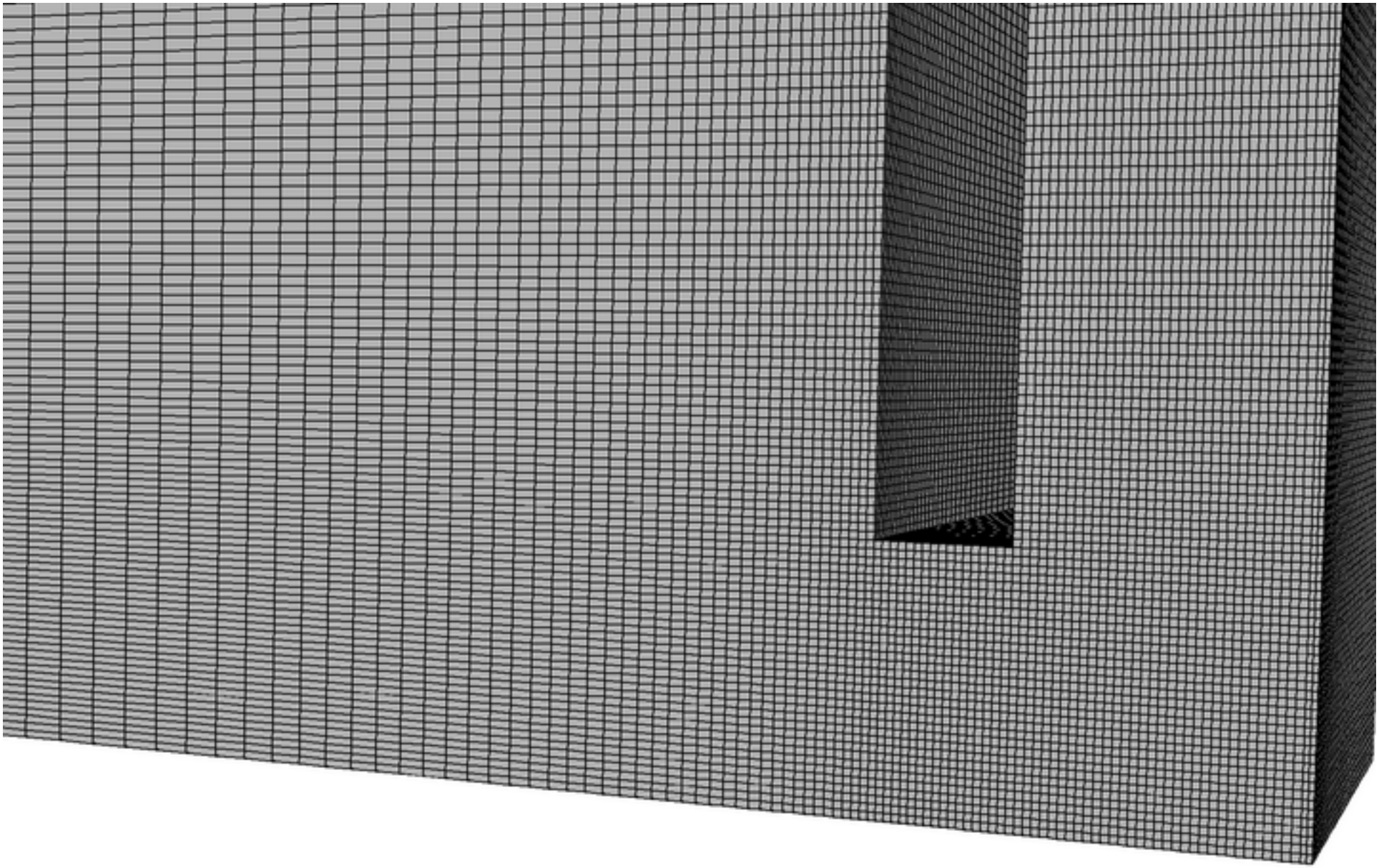

Figure(s)

Click here to download high resolution image

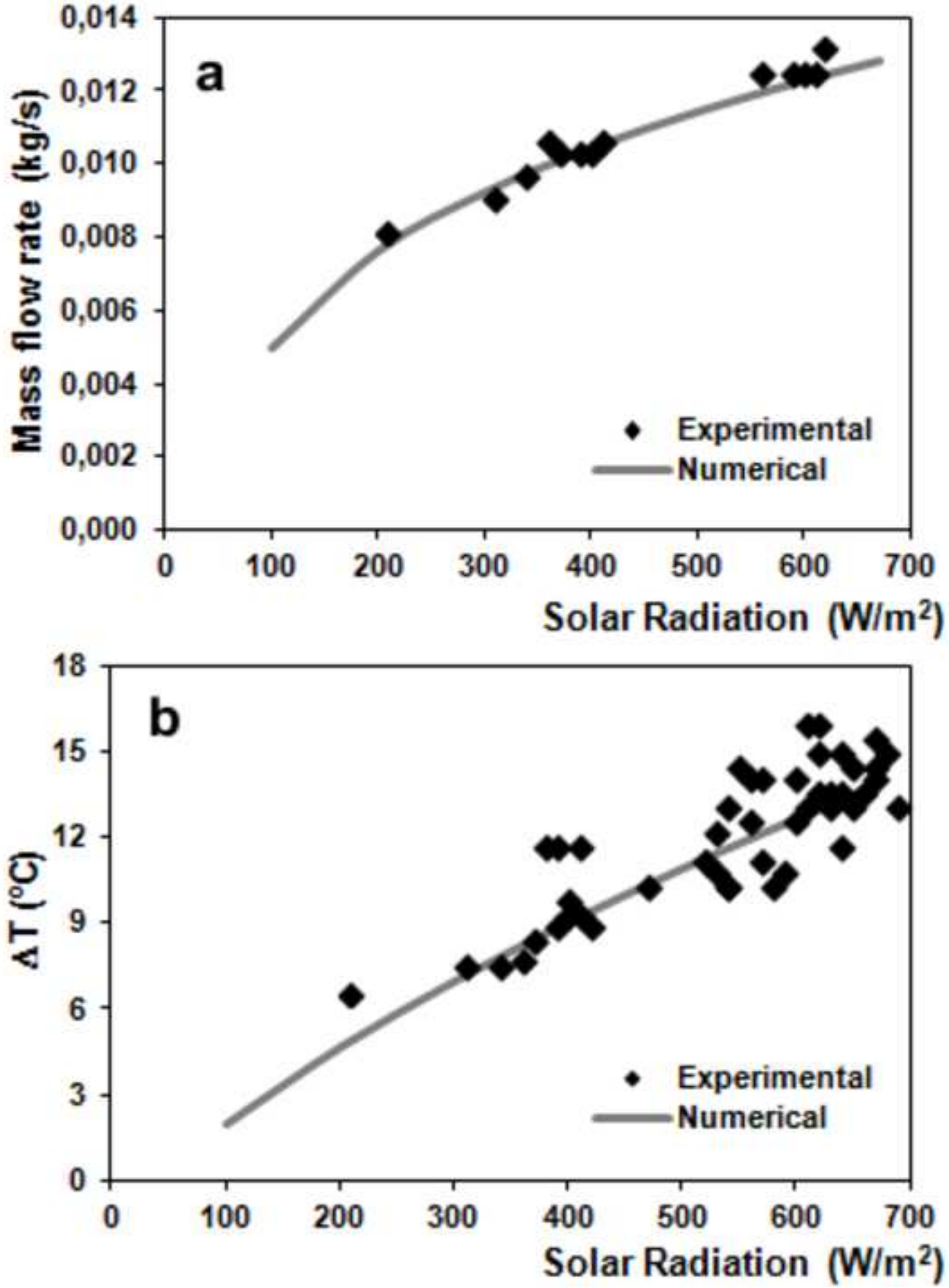

Figure(s)

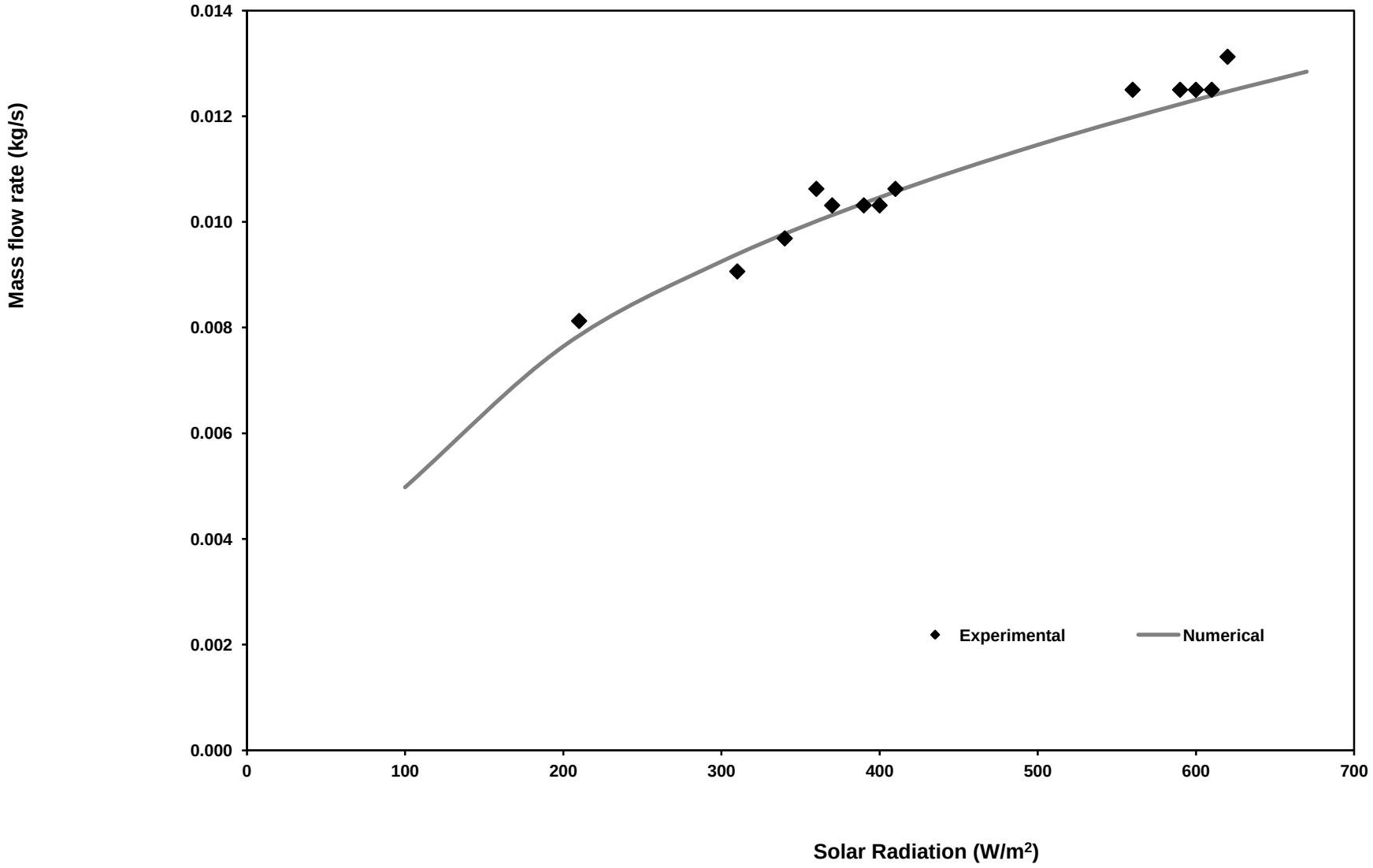
Mass flow rate (kg/s)
0.014
0.012
0.010
0.008
0.006
0.004
0.002
0.000
0
100
200
300
400
500
600
700
Experimental
Numerical
Solar Radiation (W/m2)

Figure(s)

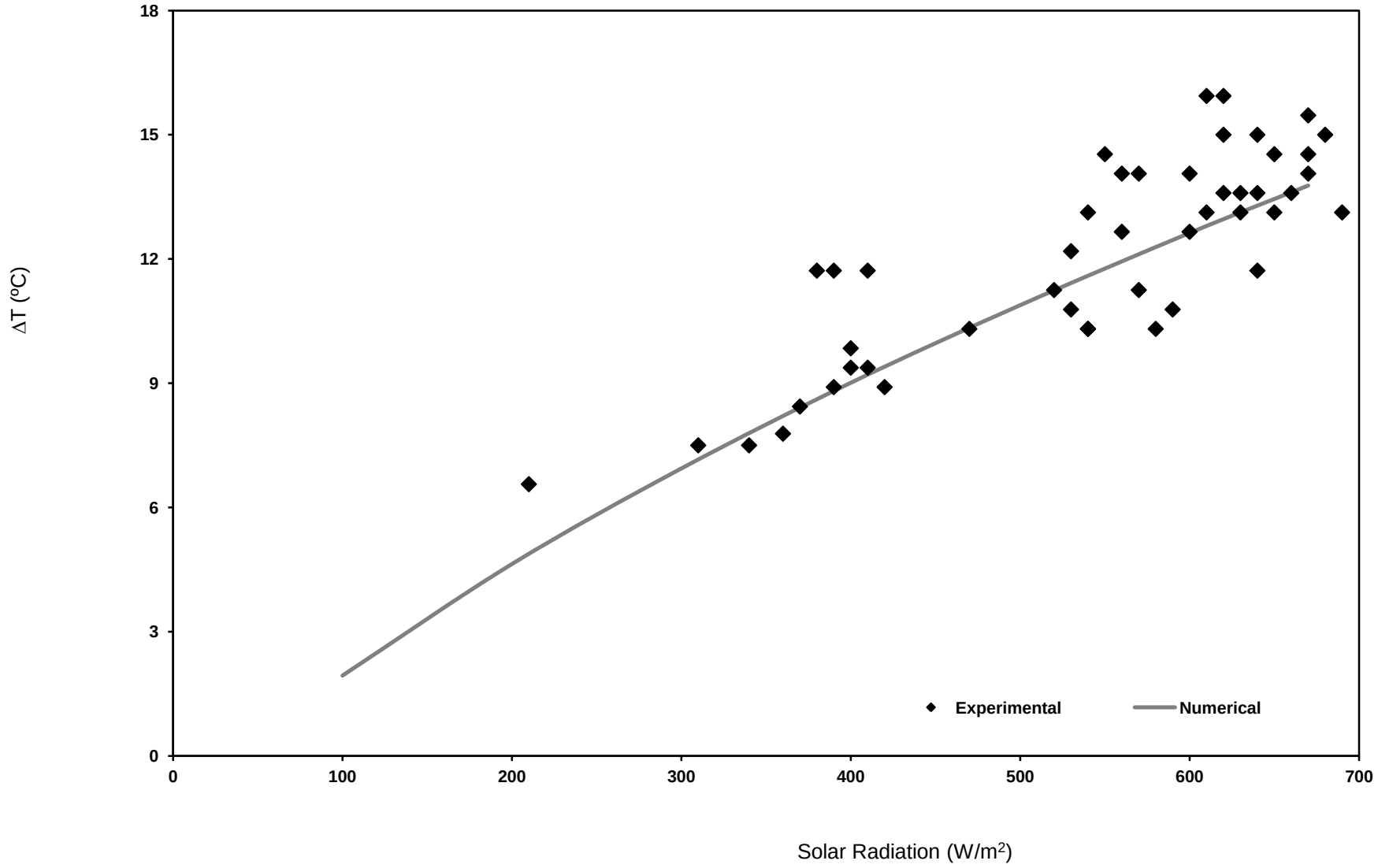
18
15
12
9
6
3
0
ΔT (°C)
0
100
200
300
400
500
600
700
Solar Radiation (W/m2)
Experimental
Numerical

Figure(s)

Click here to download high resolution image

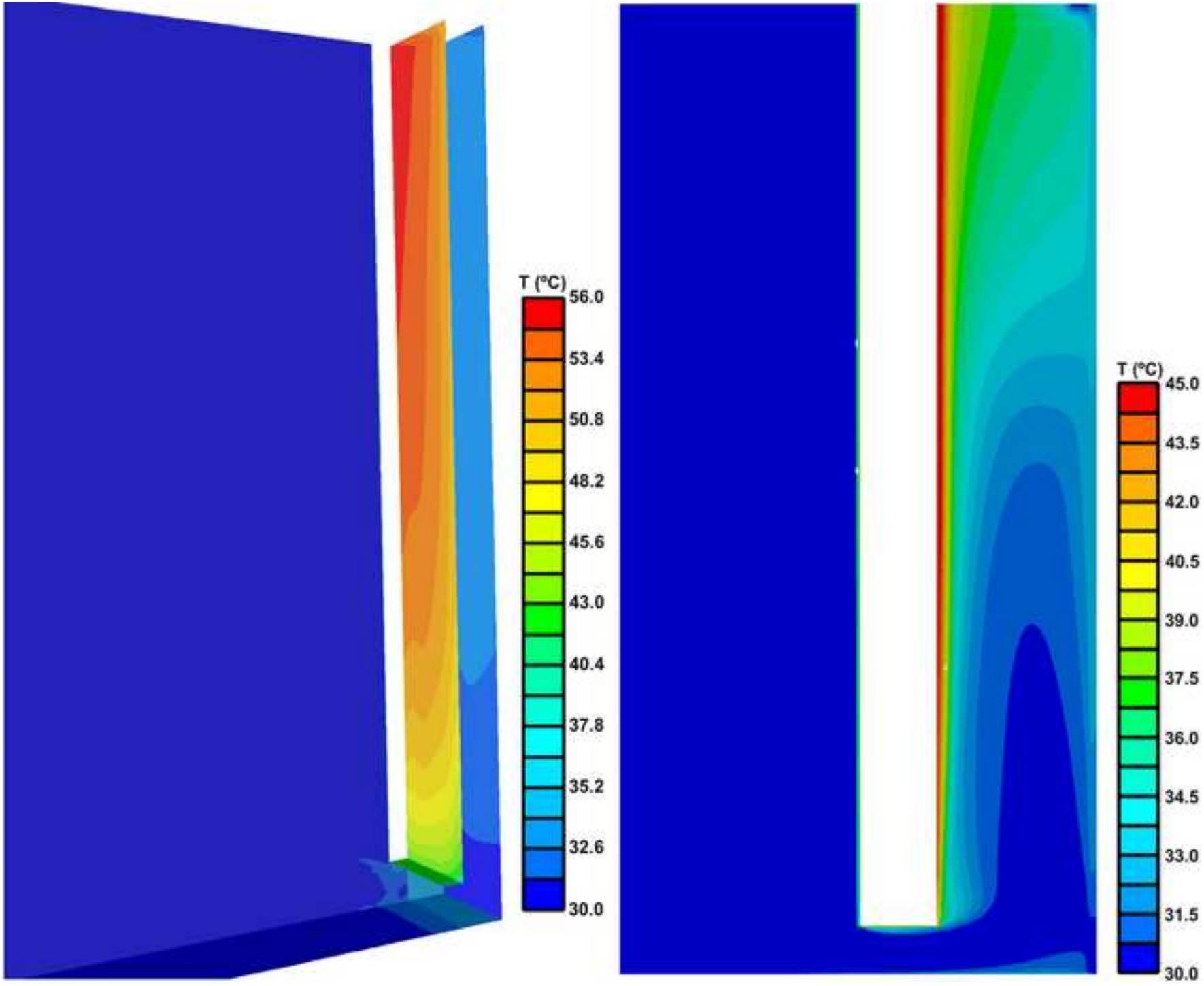

Figure(s)

Click here to download high resolution image

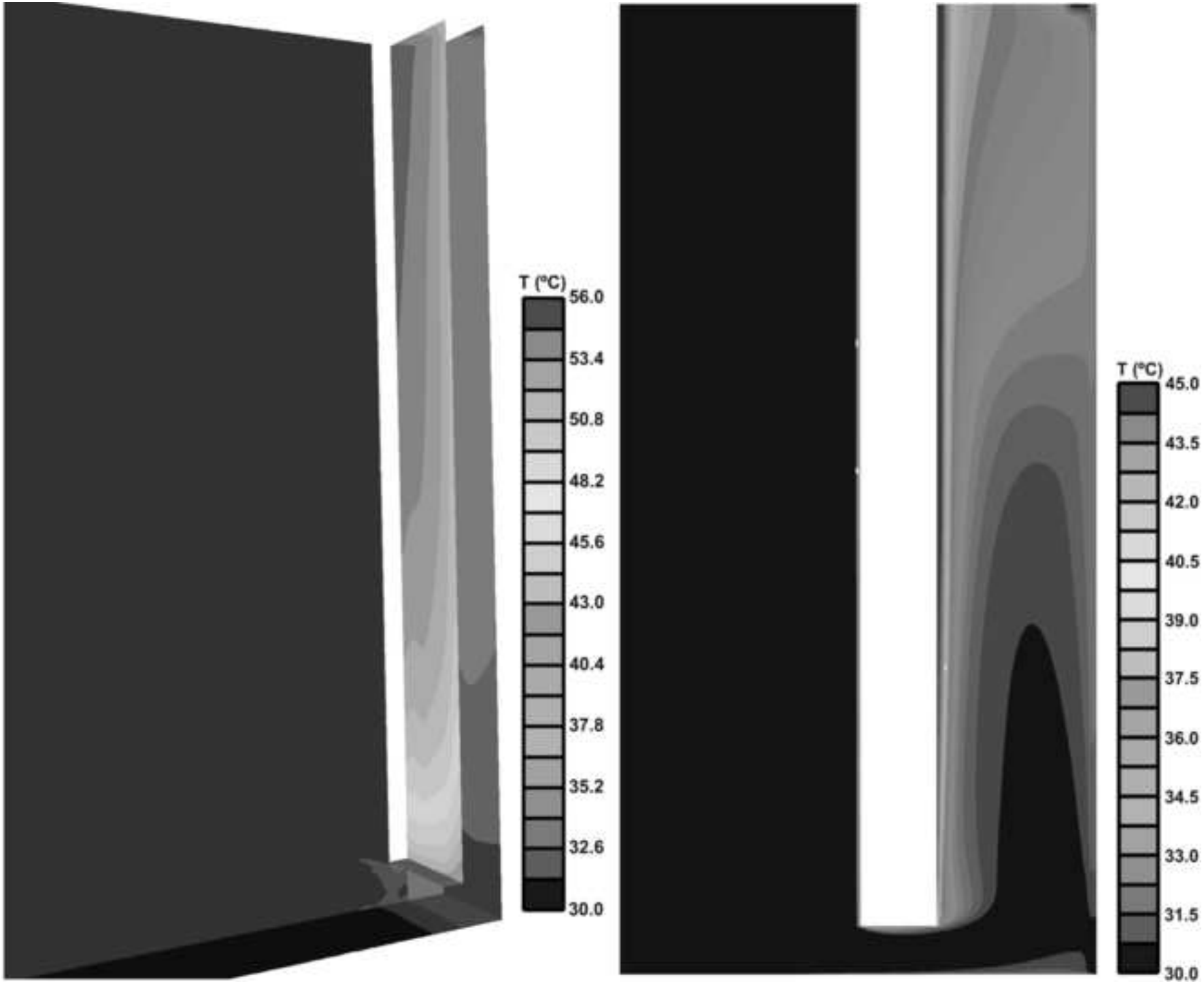

Figure(s)

Click here to download high resolution image

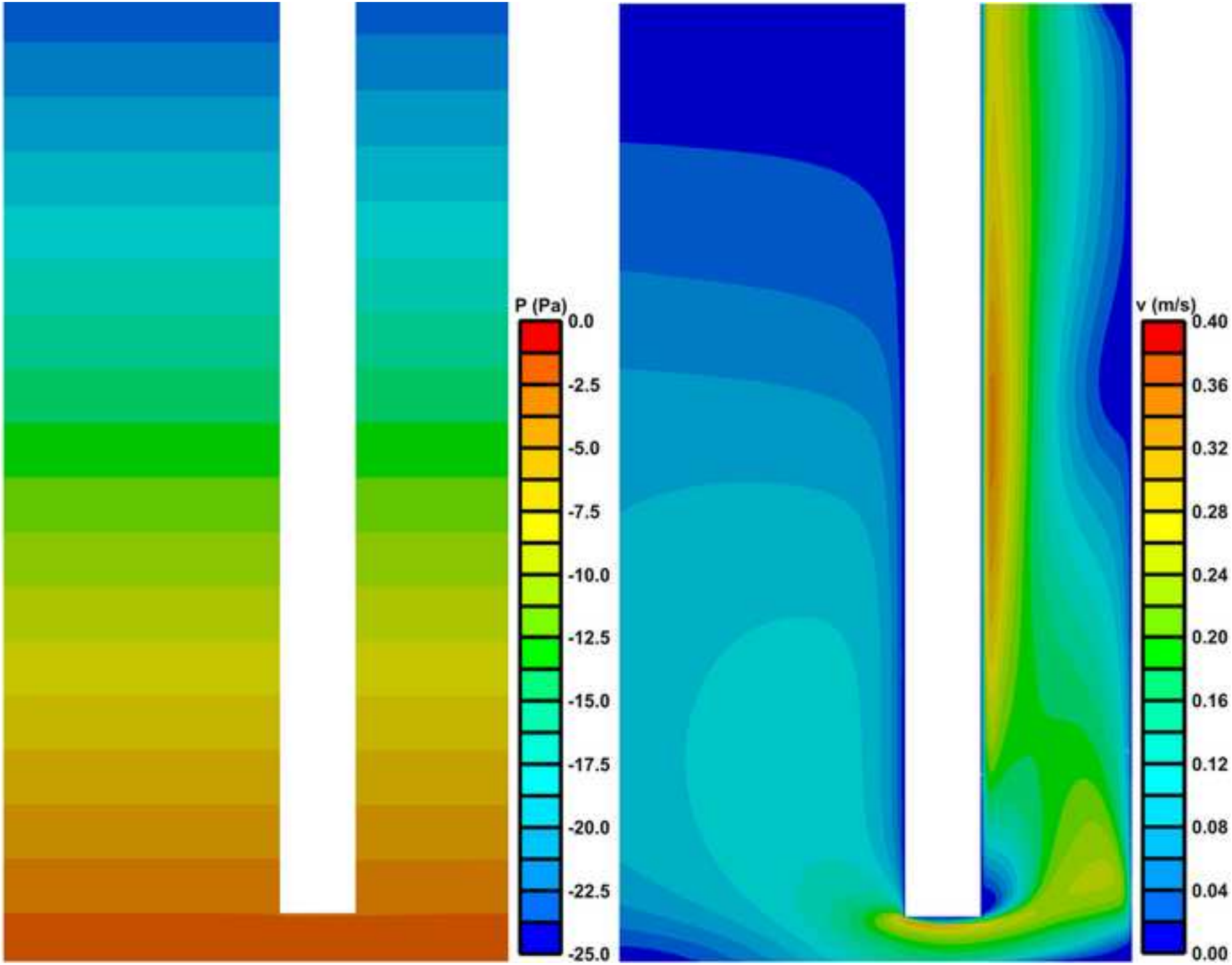

Figure(s)

Click here to download high resolution image

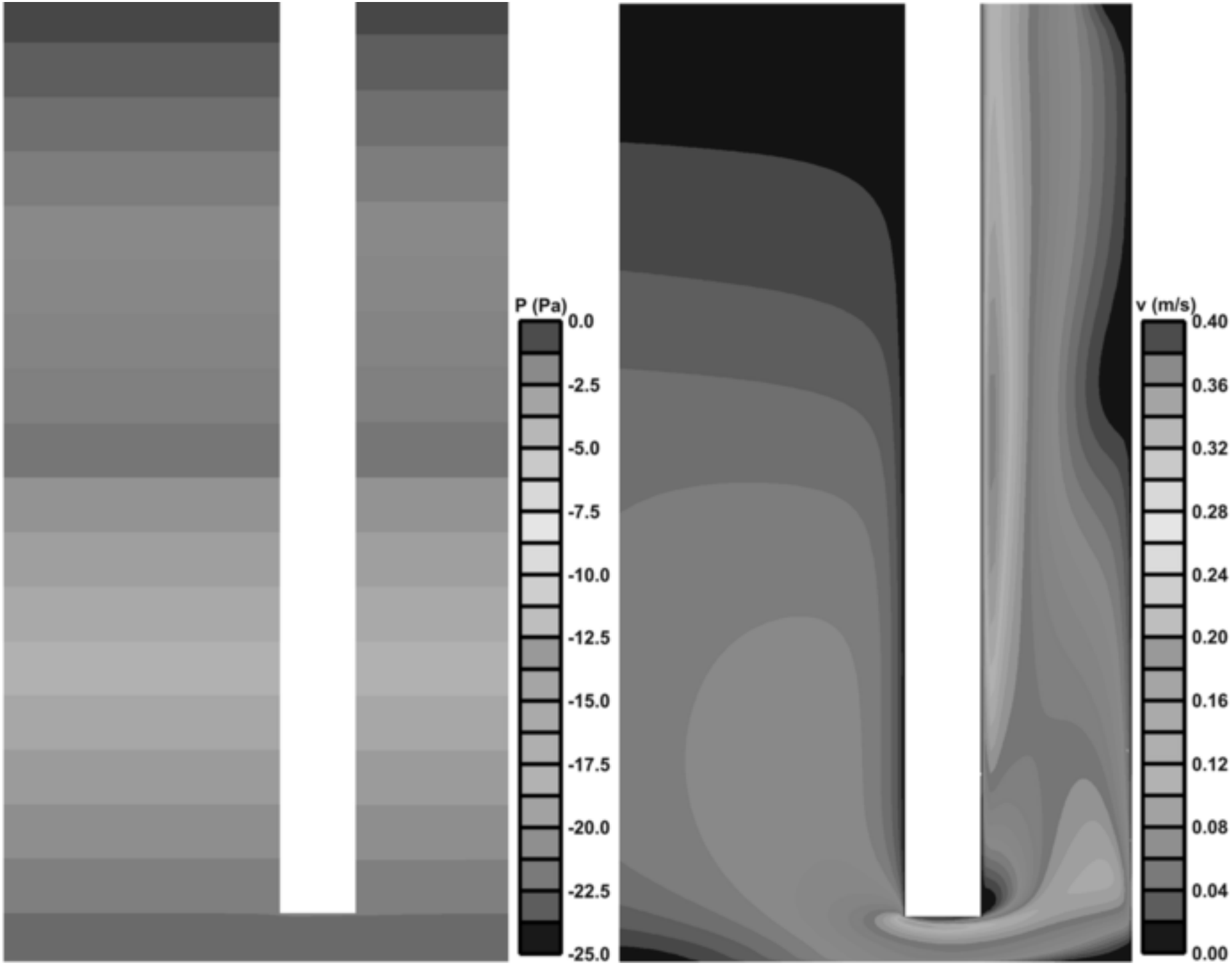

Figure(s)

Click here to download high resolution image

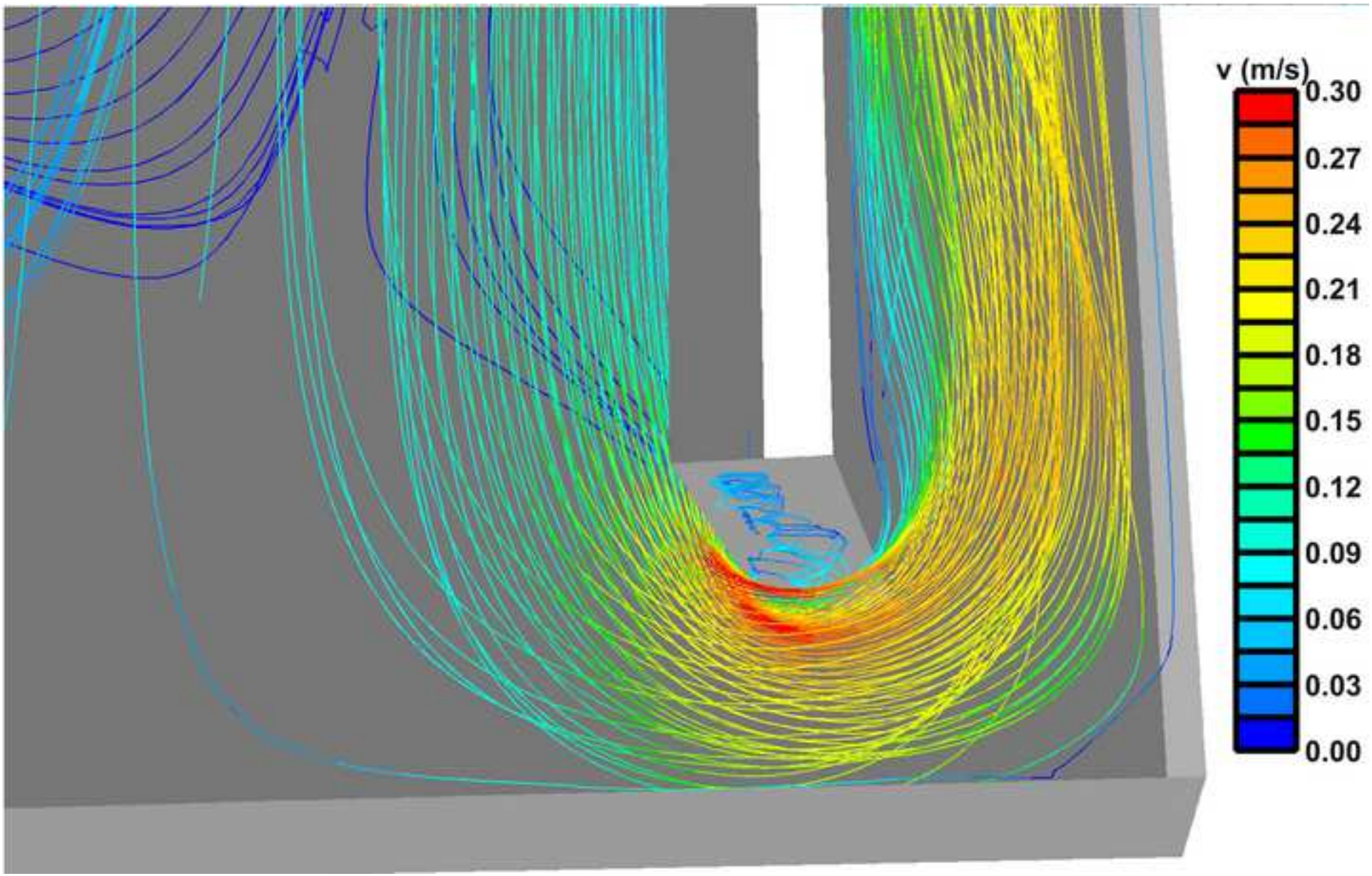

Figure(s)

Click here to download high resolution image

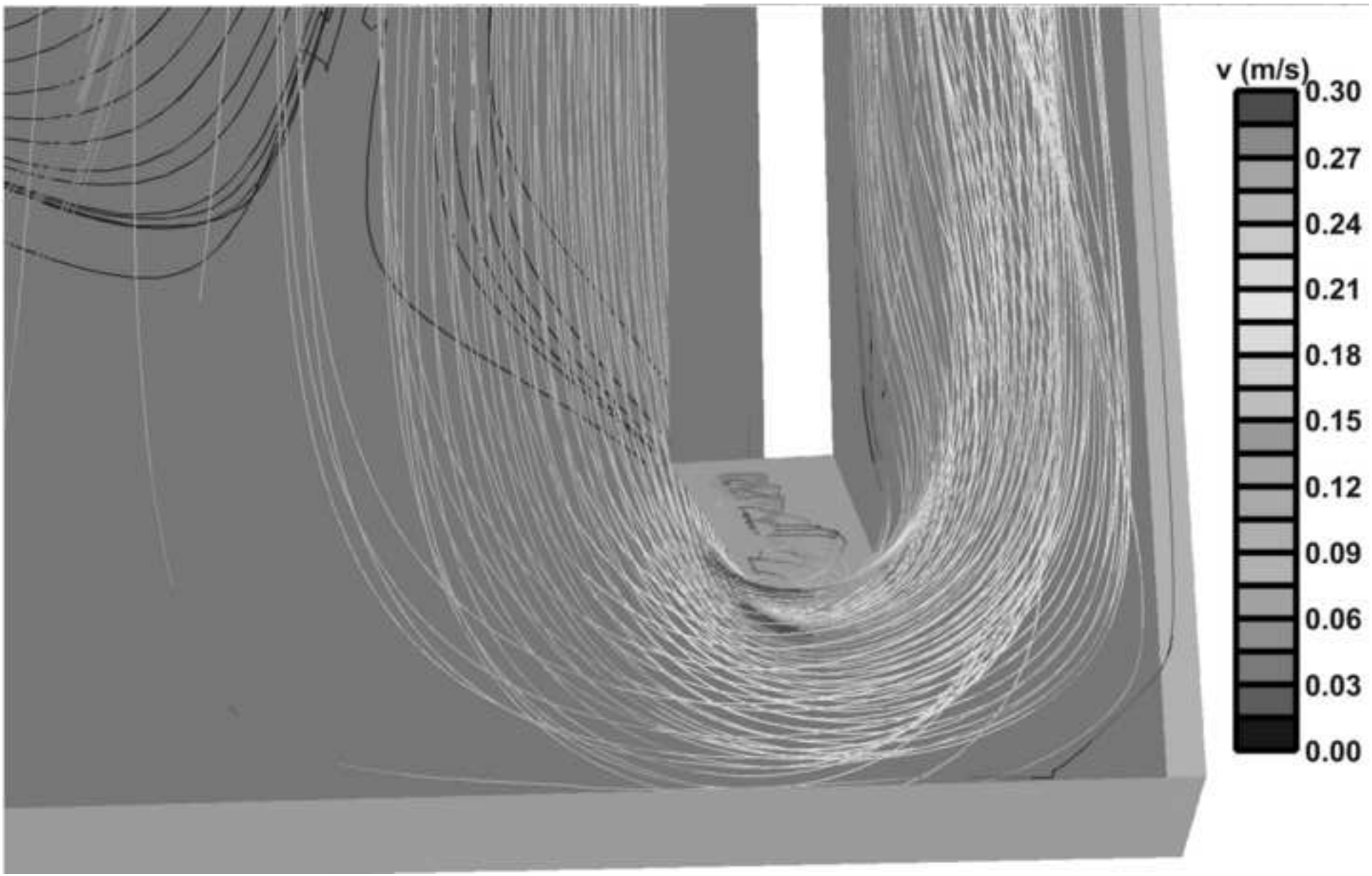

Figure(s)

Click here to download high resolution image

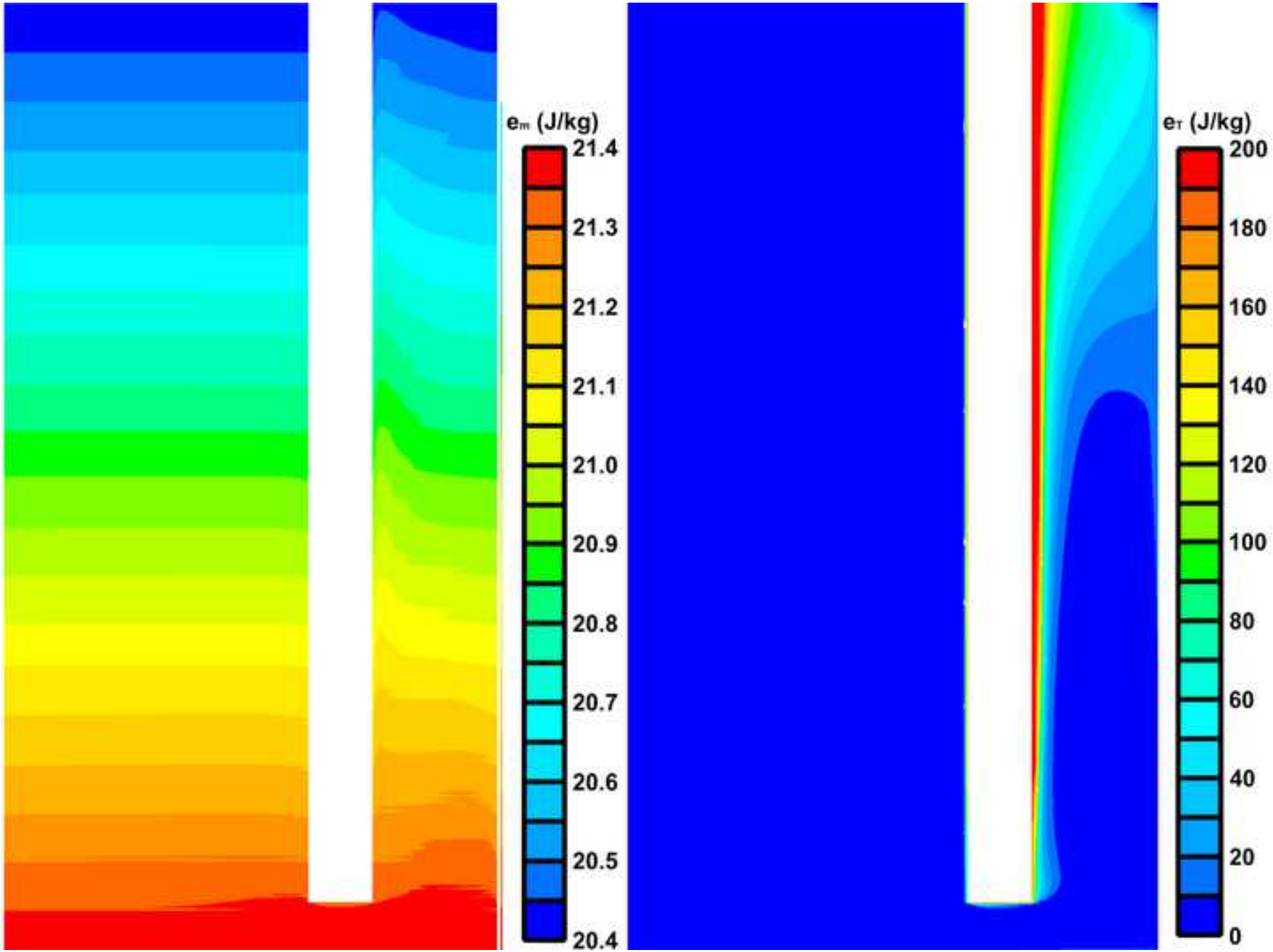

Figure(s)

Click here to download high resolution image

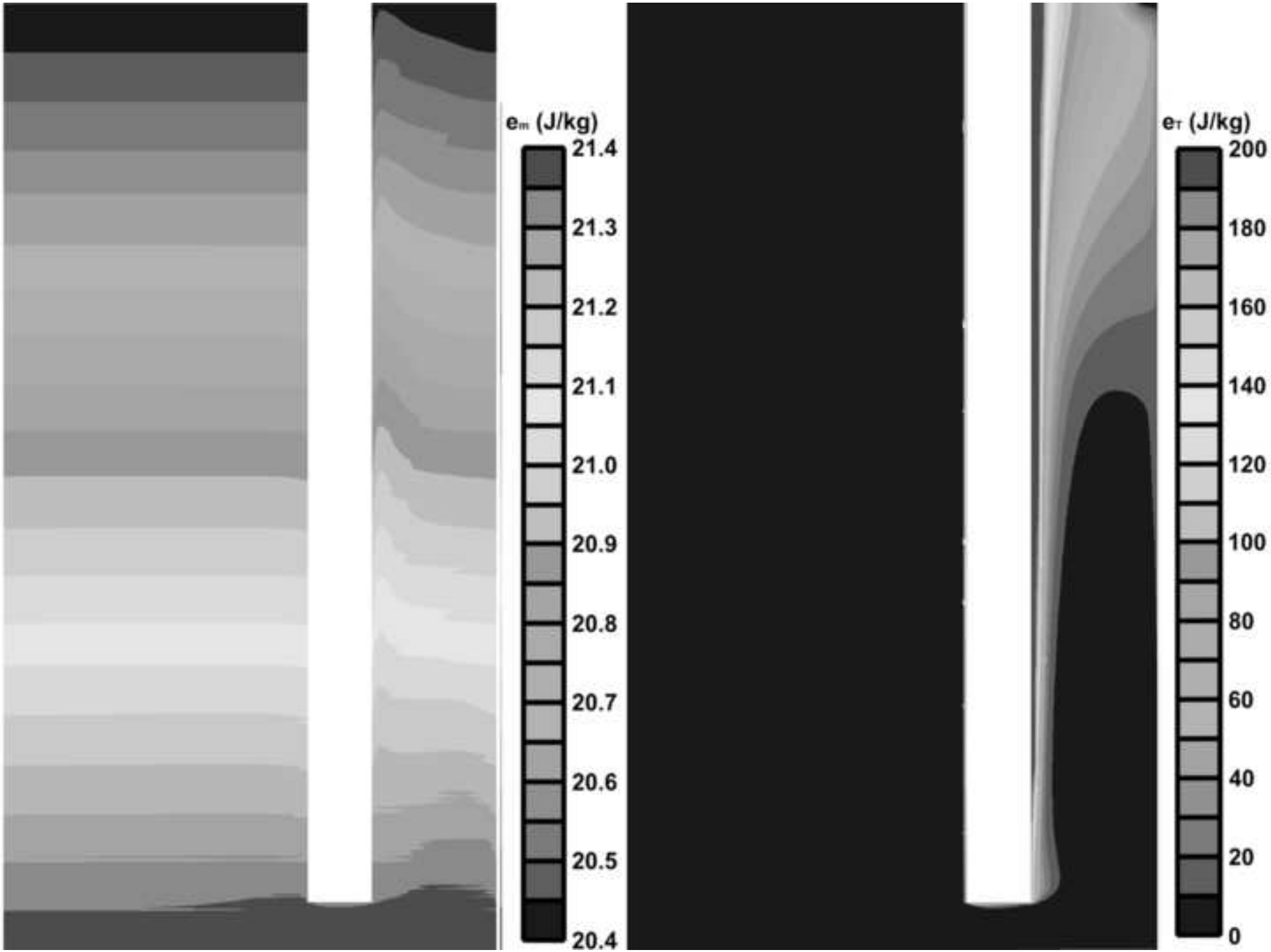

Figure(s)

Click here to download high resolution image

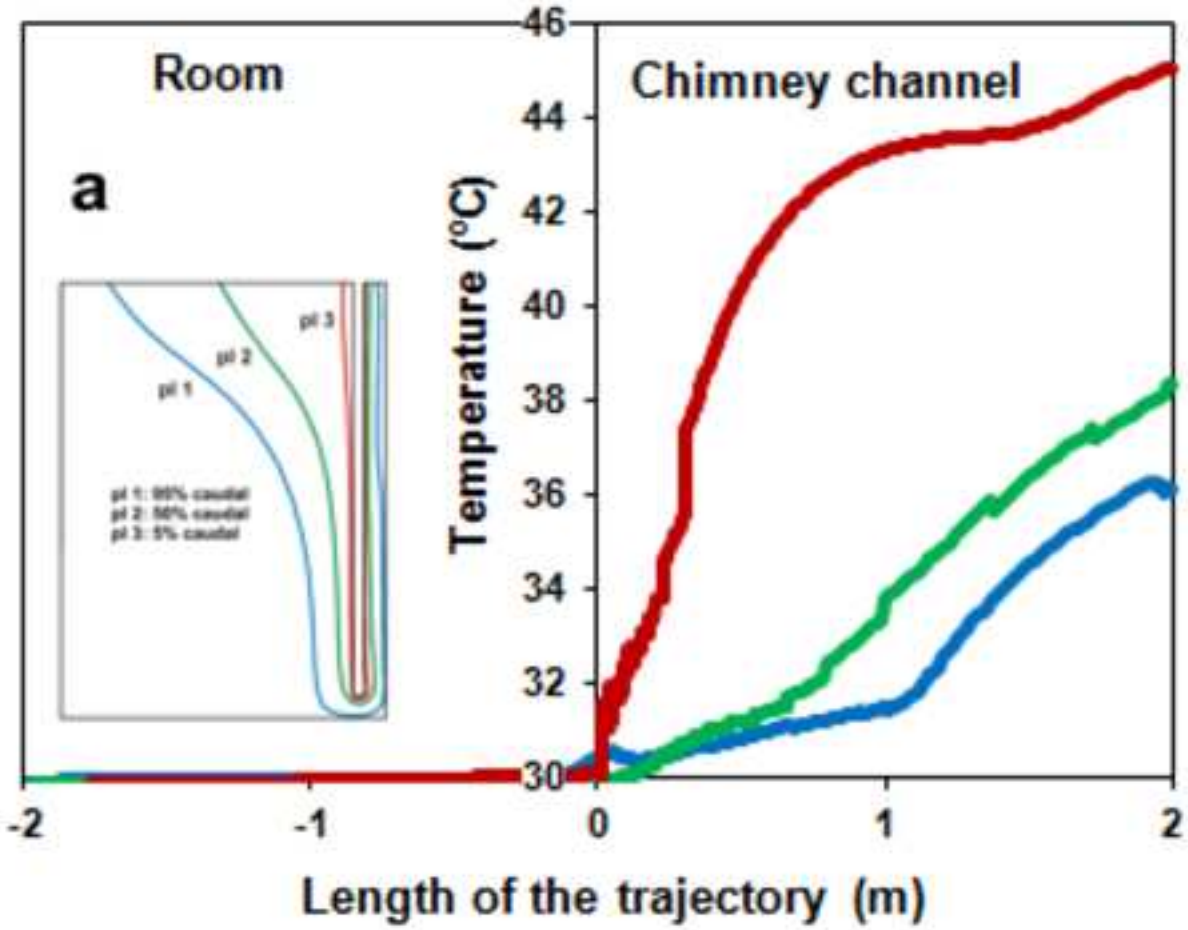

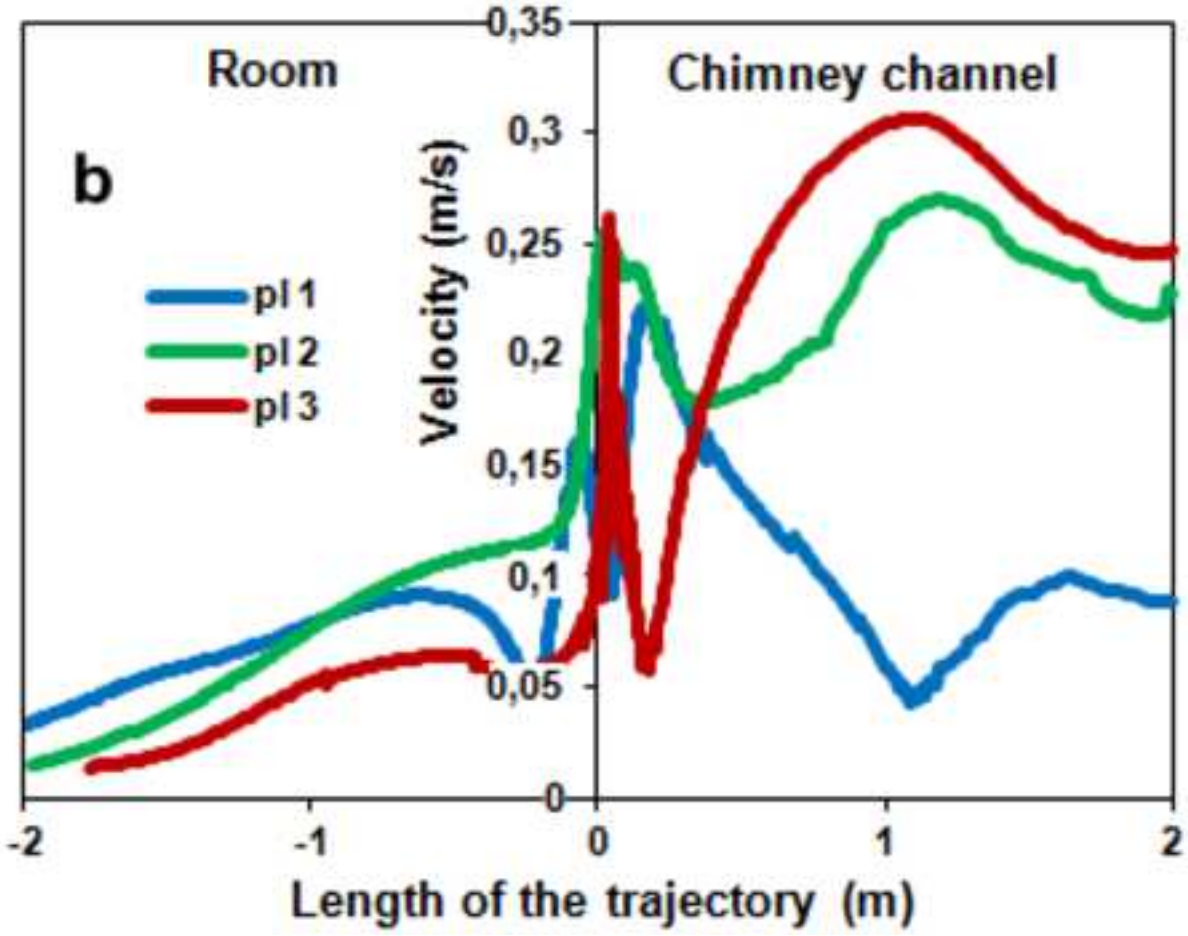

Figure(s)

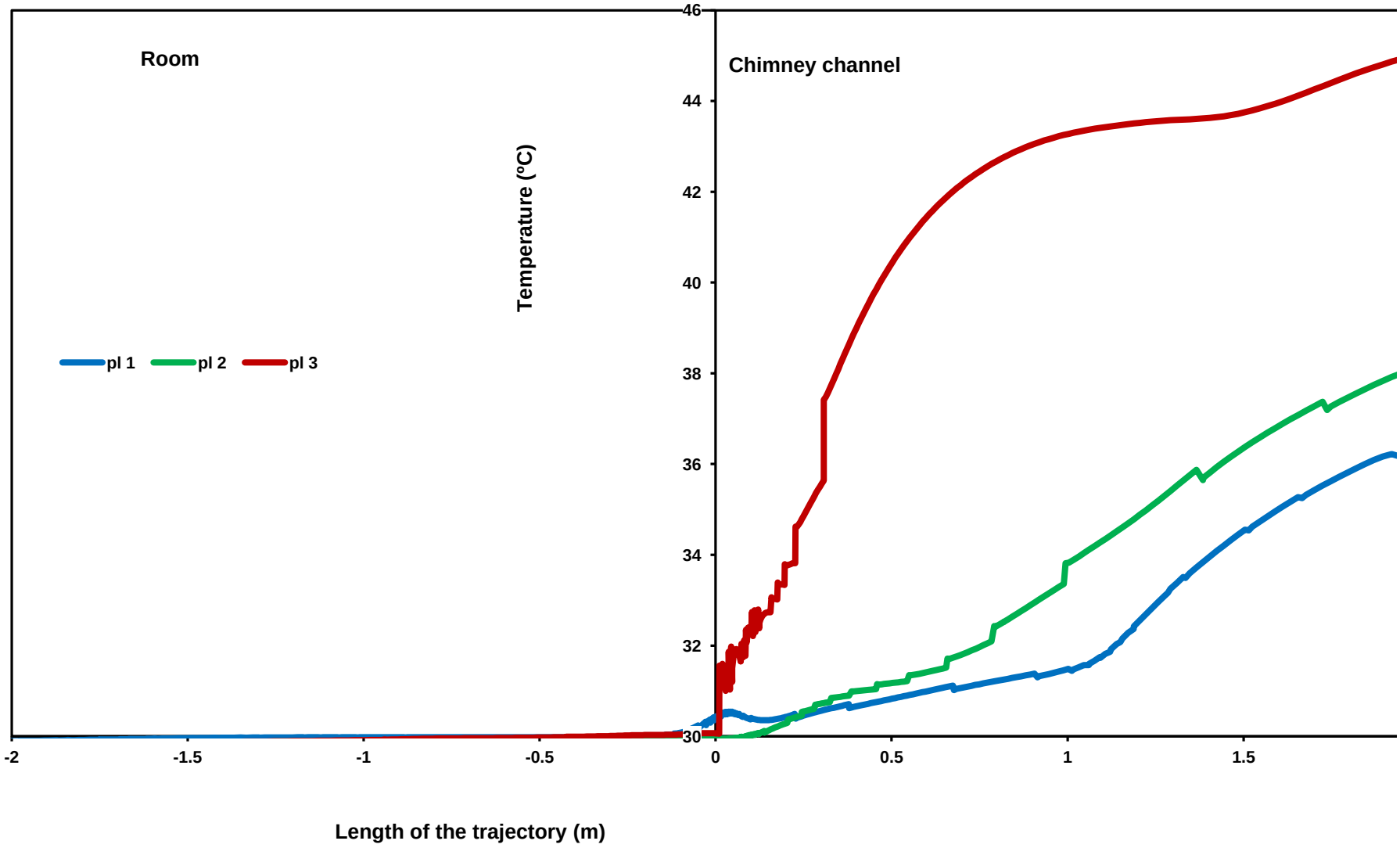
Room
Chimney channel
Temperature (°C)
pl 1
pl 2
pl 3
46
44
42
40
38
36
34
32
30
-2
-1.5
-1
-0.5
0
0.5
1
1.5
Length of the trajectory (m)

Figure(s)

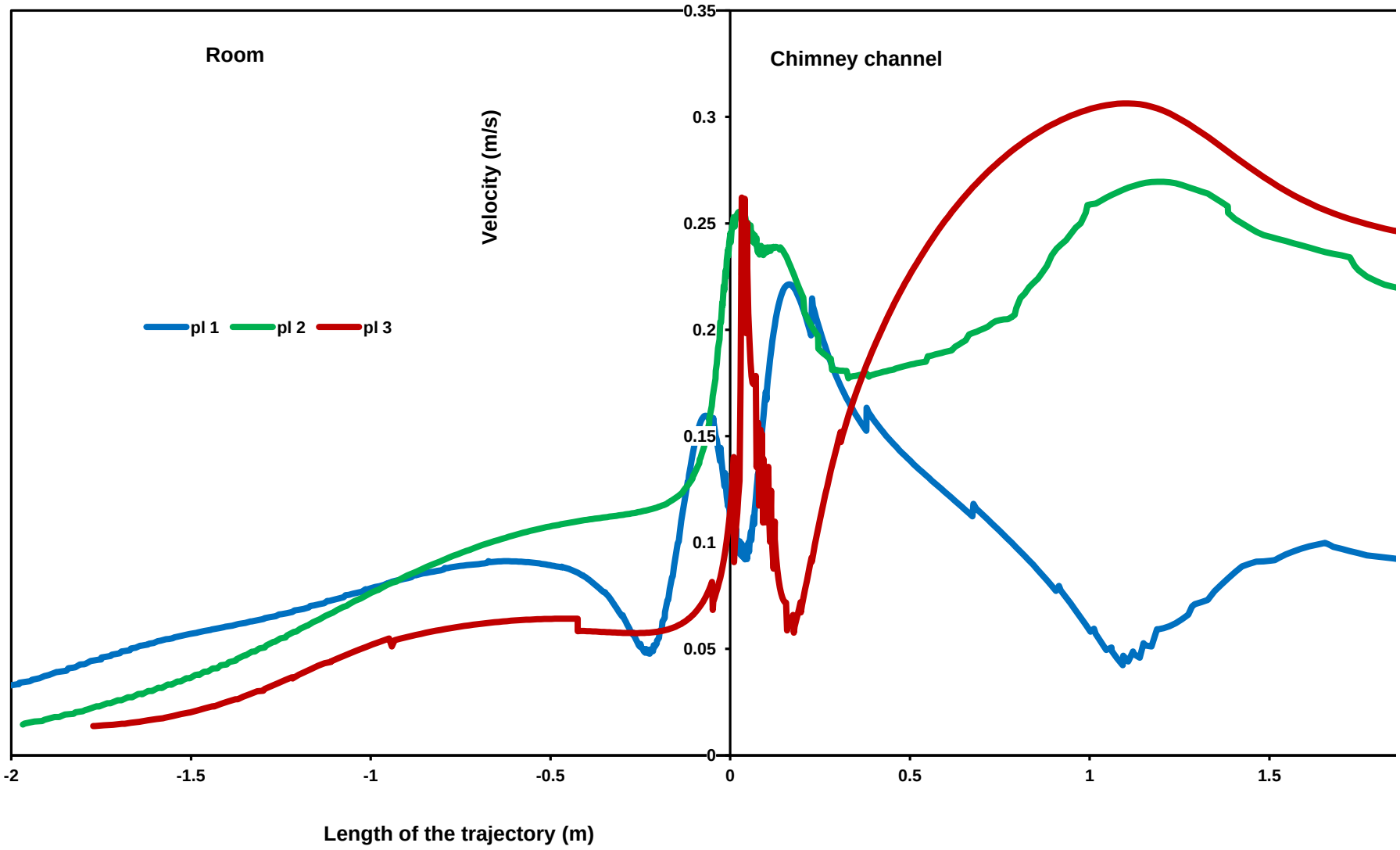
Room
Chimney channel
Velocity (m/s)
pl 1
pl 2
pl 3
0.35
0.3
0.25
0.2
0.15
0.1
0.05
0
-2
-1.5
-1
-0.5
0
0.5
1
1.5
Length of the trajectory (m)

Figure(s)

Click here to download high resolution image

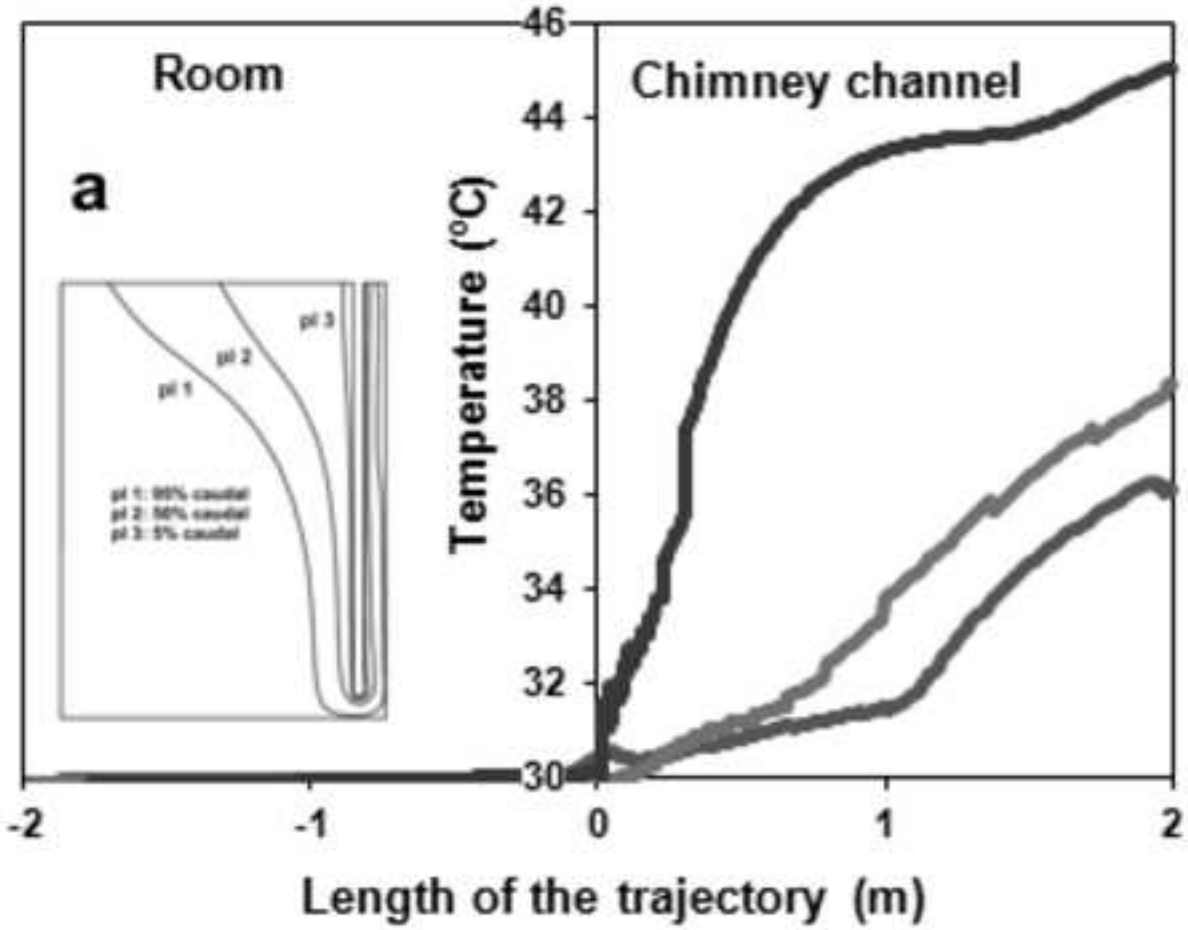

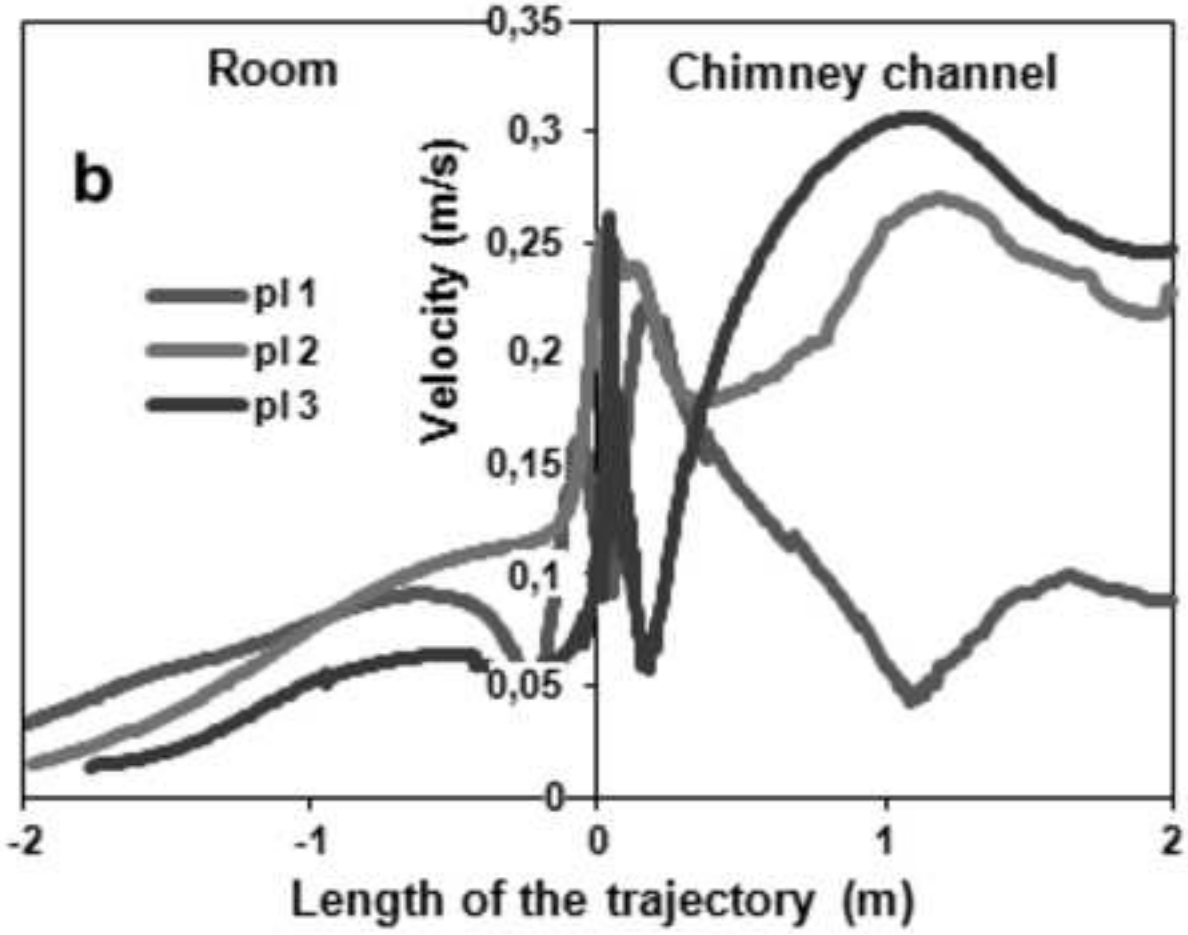

Figure(s)

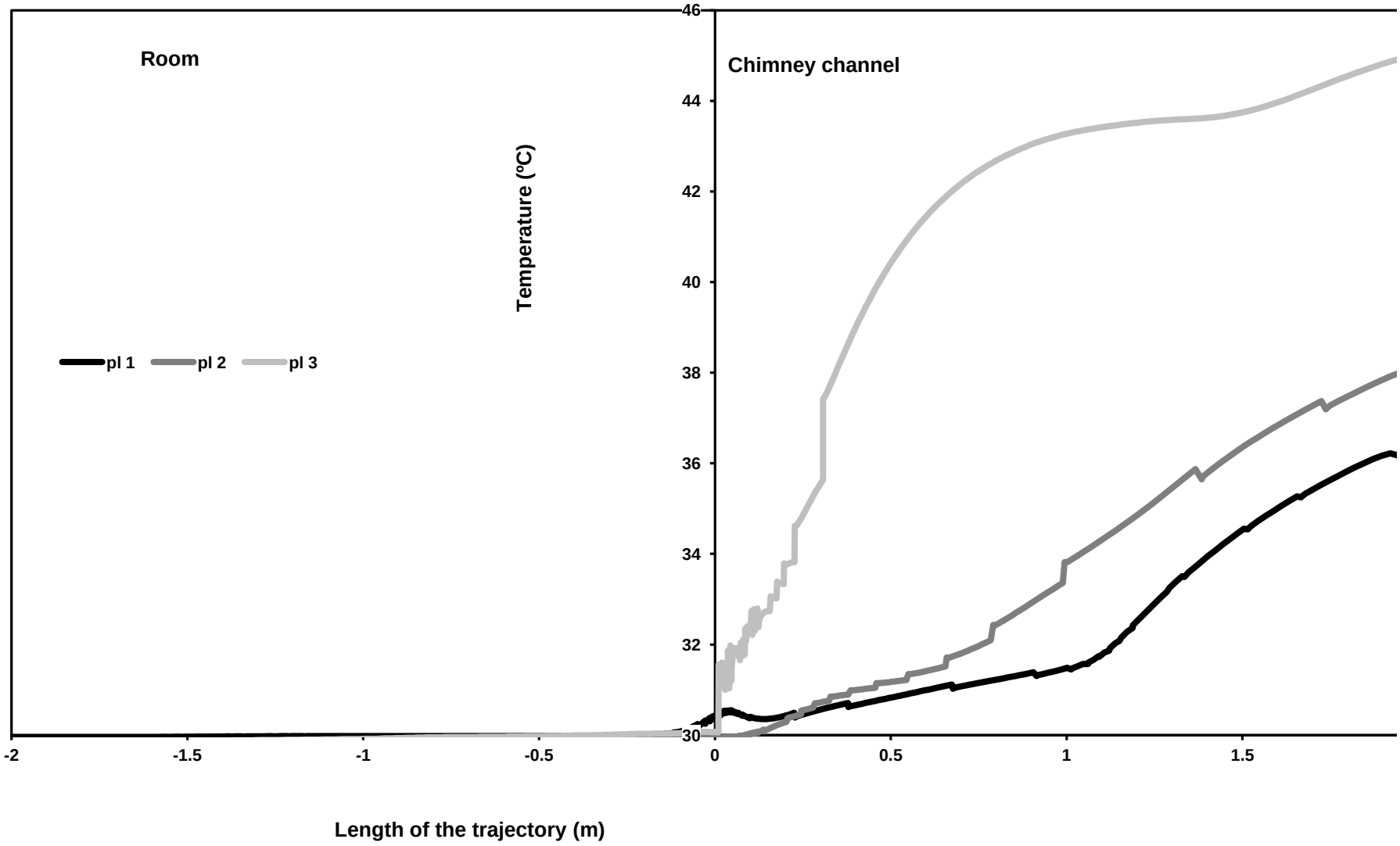
Room
Chimney channel
Temperature (°C)
pl 1
pl 2
pl 3
46
44
42
40
38
36
34
32
30
-2
-1.5
-1
-0.5
0
0.5
1
1.5
Length of the trajectory (m)

Figure(s)

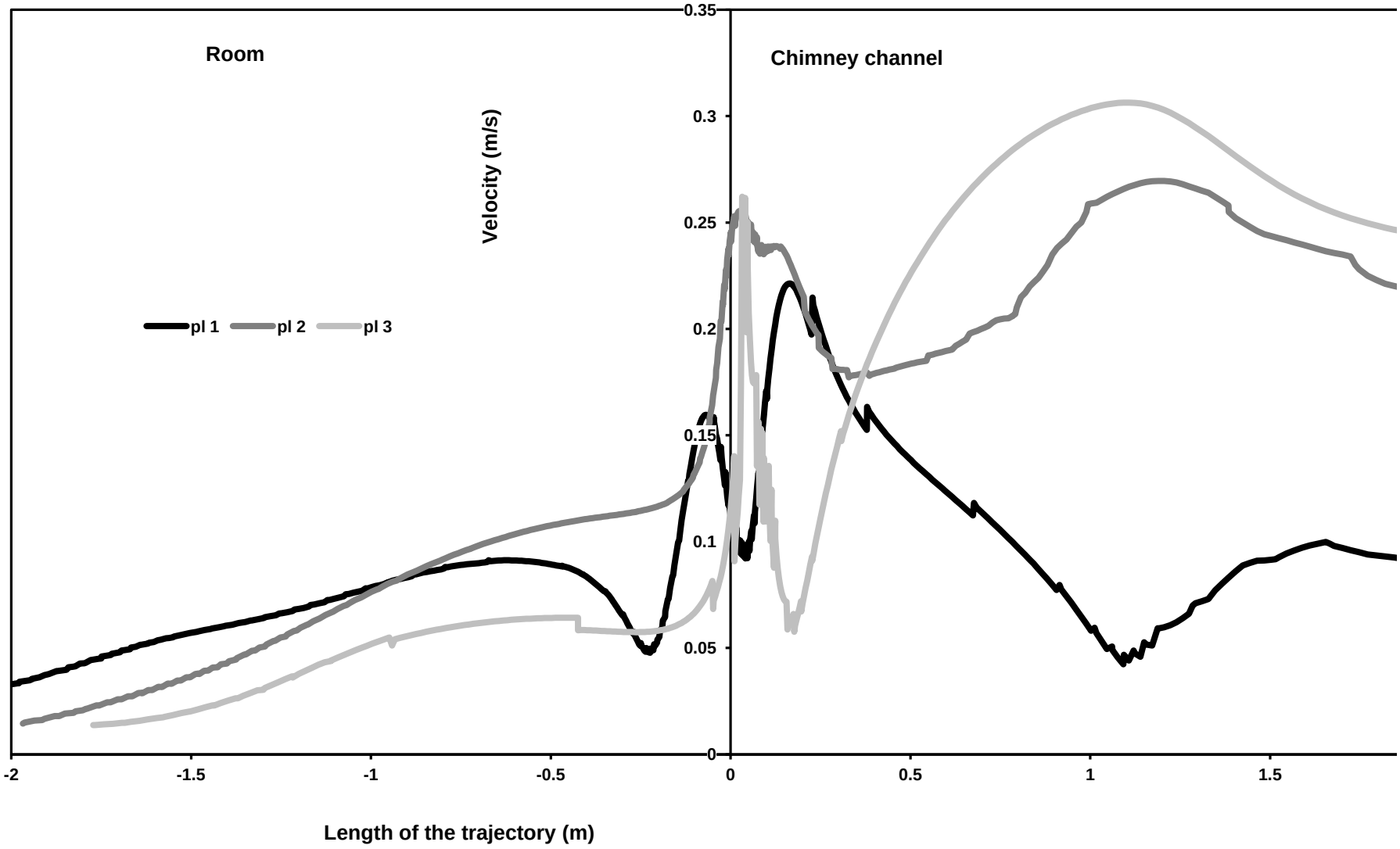
Room
Chimney channel
Velocity (m/s)
pl 1
pl 2
pl 3
0.35
0.3
0.25
0.2
0.15
0.1
0.05
0
-2
-1.5
-1
-0.5
0
0.5
1
1.5
Length of the trajectory (m)

Figure(s)

Click here to download high resolution image

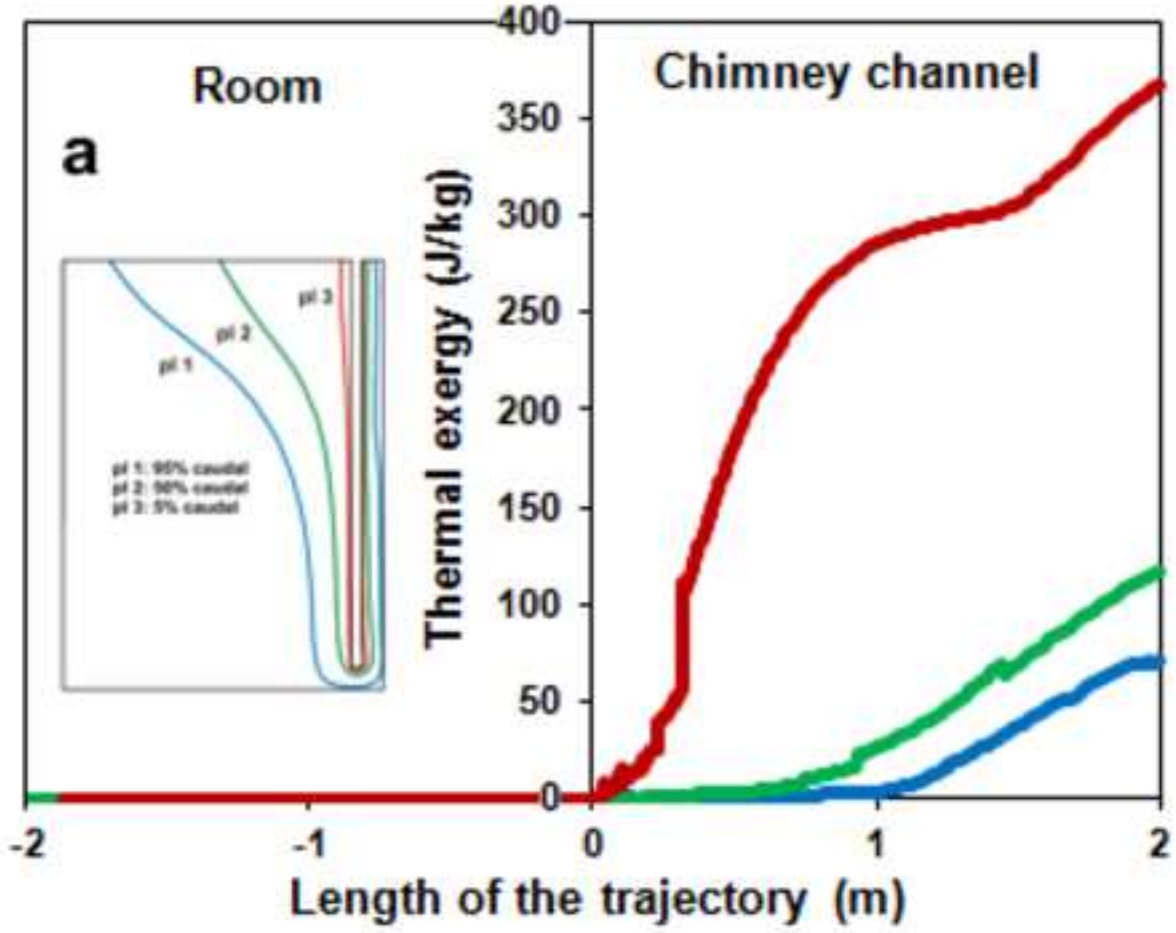

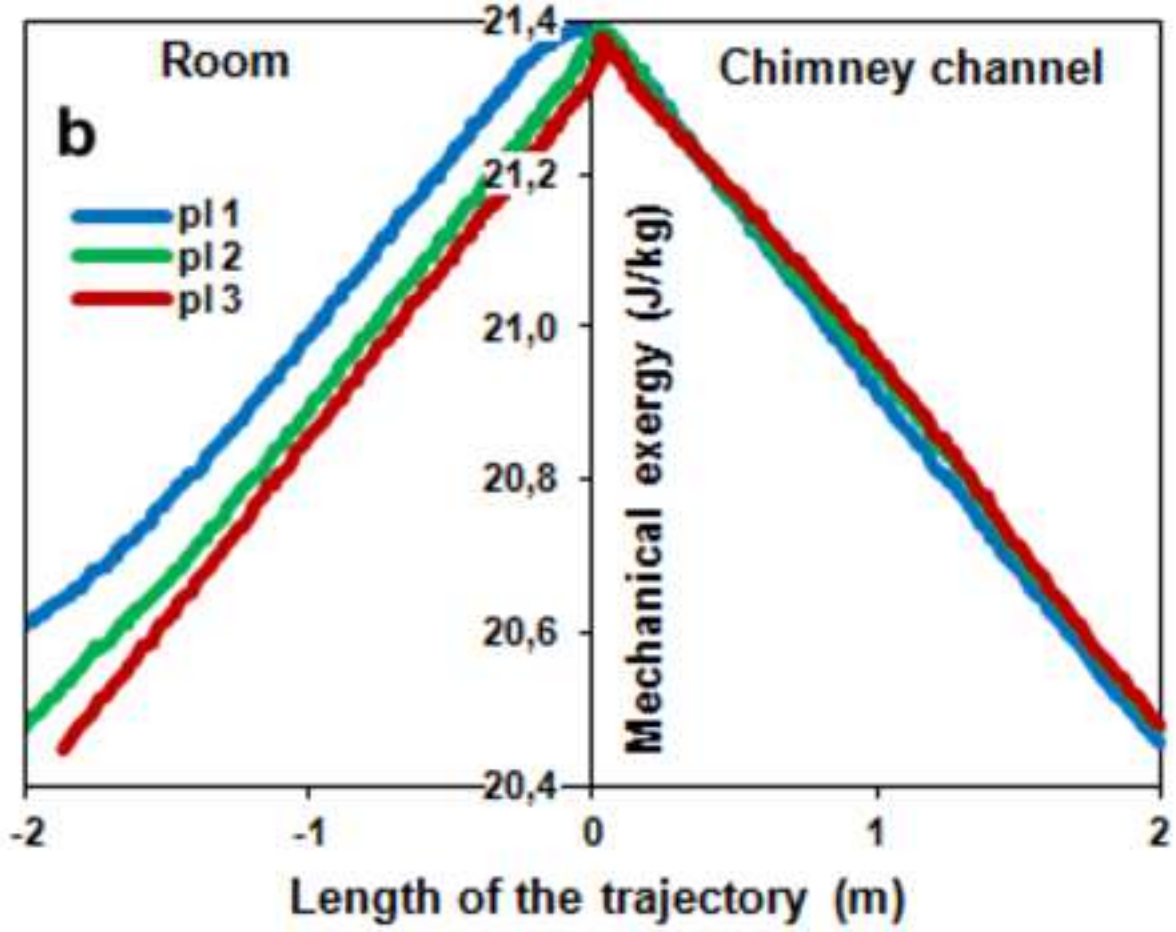

Figure(s)

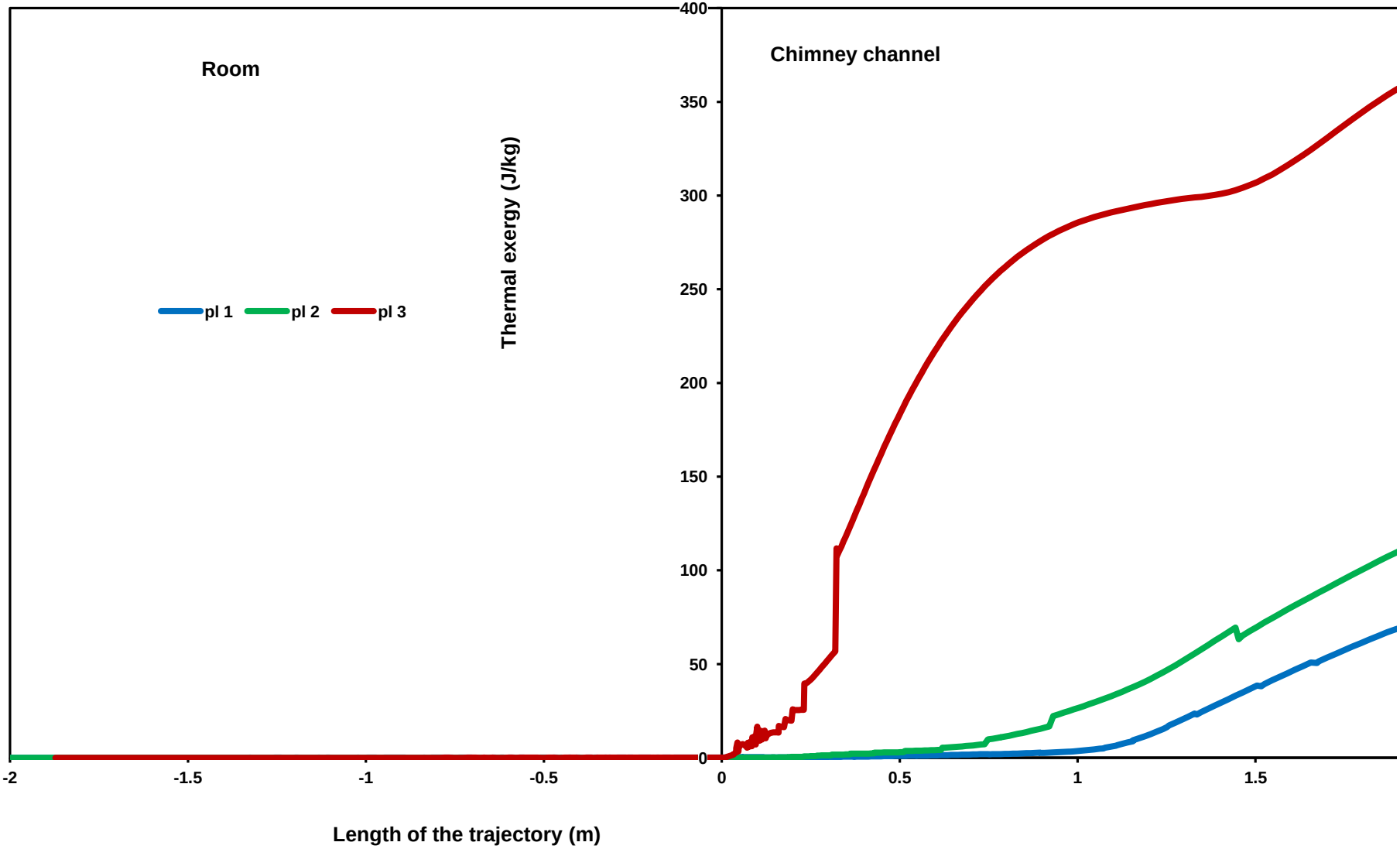
Room
Chimney channel
pl 1
pl 2
pl 3
Thermal exergy (J/kg)
400
350
300
250
200
150
100
50
0
-2
-1.5
-1
-0.5
0
0.5
1
1.5
Length of the trajectory (m)

Figure(s)

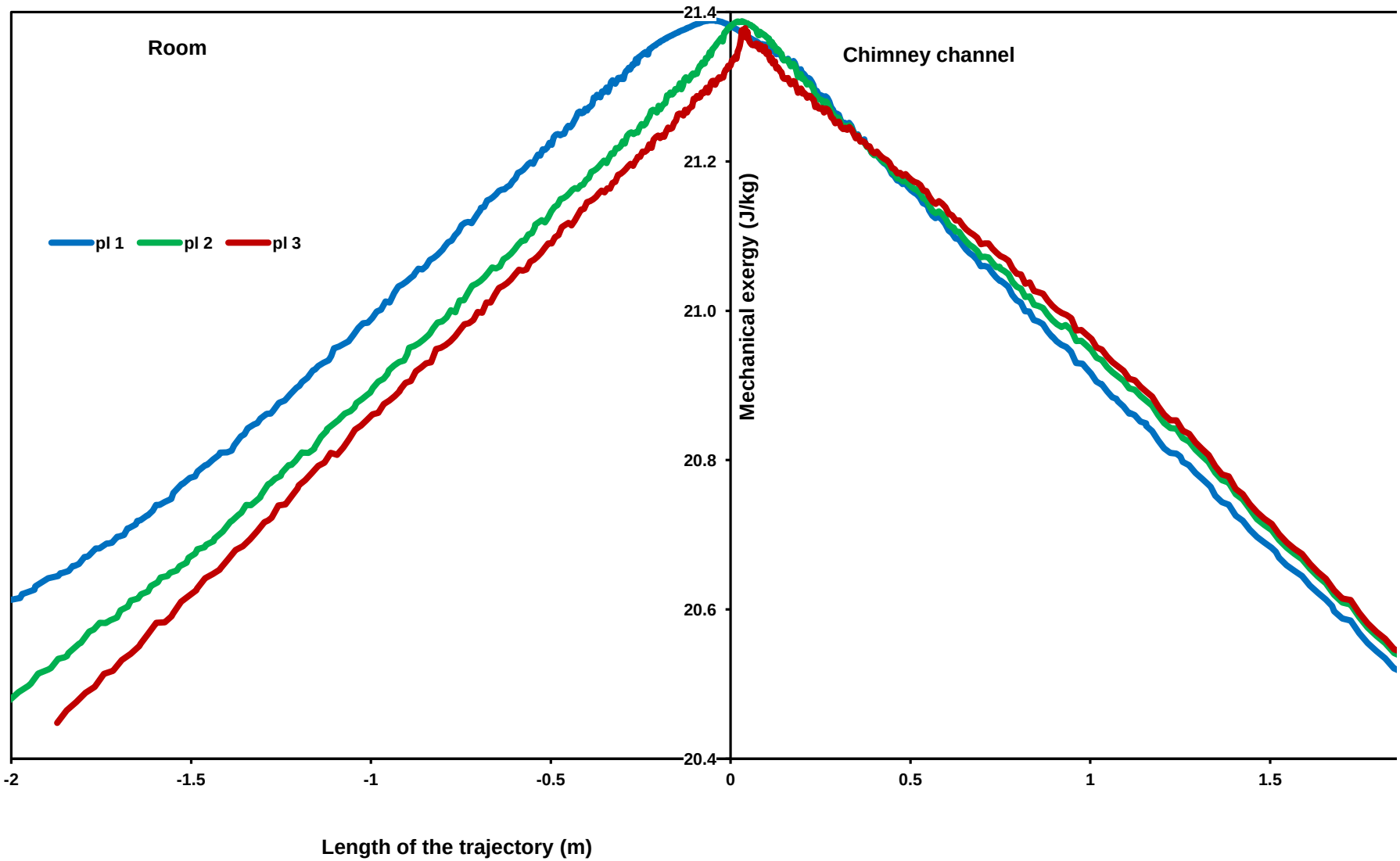
Room
Chimney channel
pl 1
pl 2
pl 3
Mechanical exergy (J/kg)
21.4
21.2
21.0
20.8
20.6
20.4
-2
-1.5
-1
-0.5
0
0.5
1
1.5
Length of the trajectory (m)

Figure(s)

Click here to download high resolution image

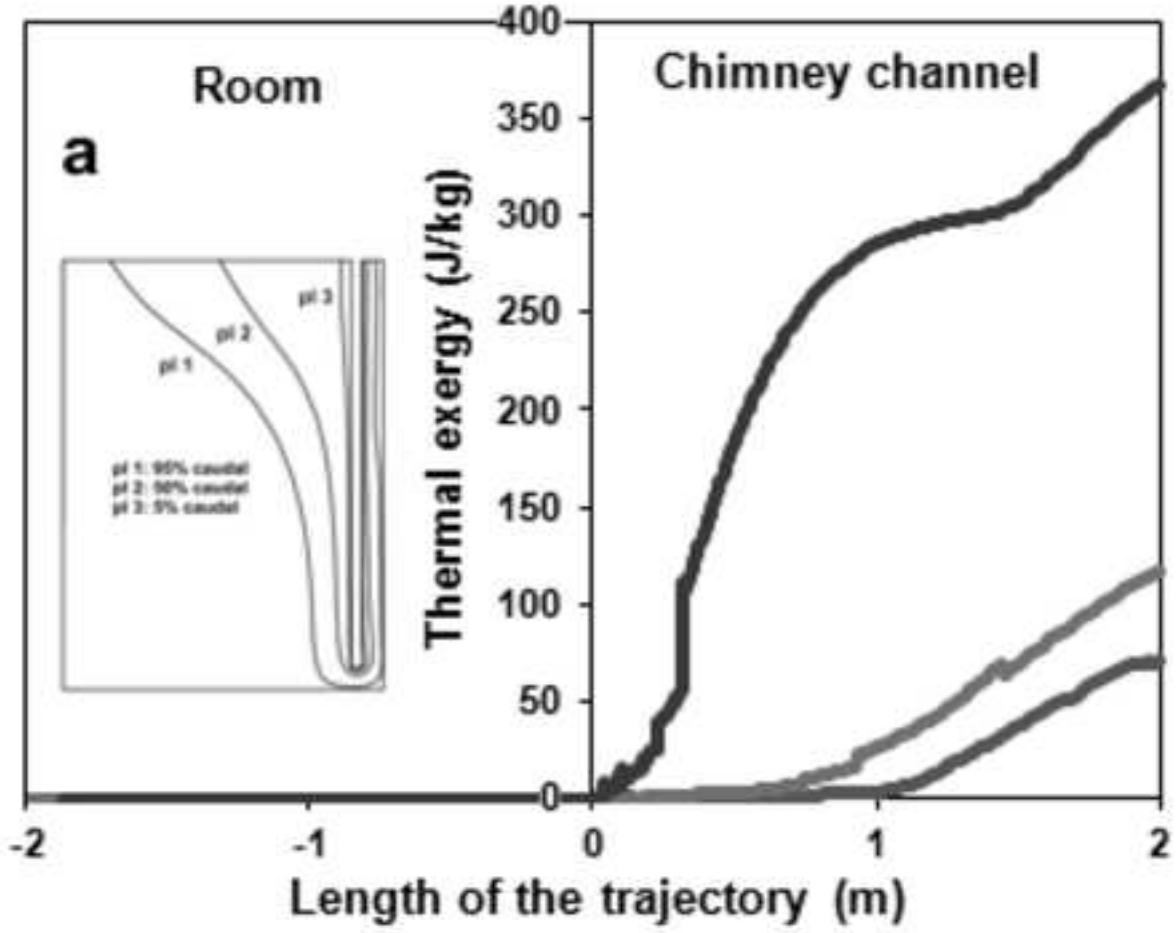

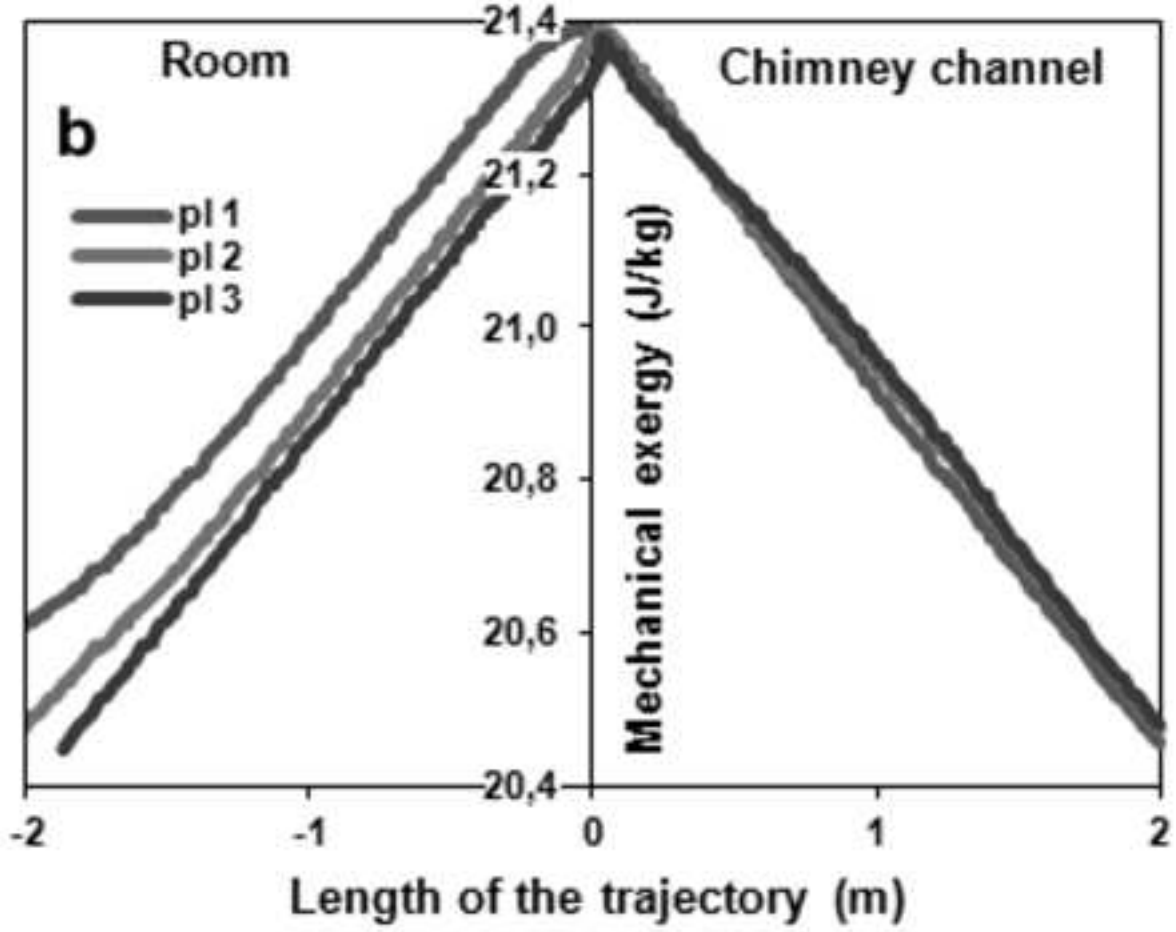

Figure(s)

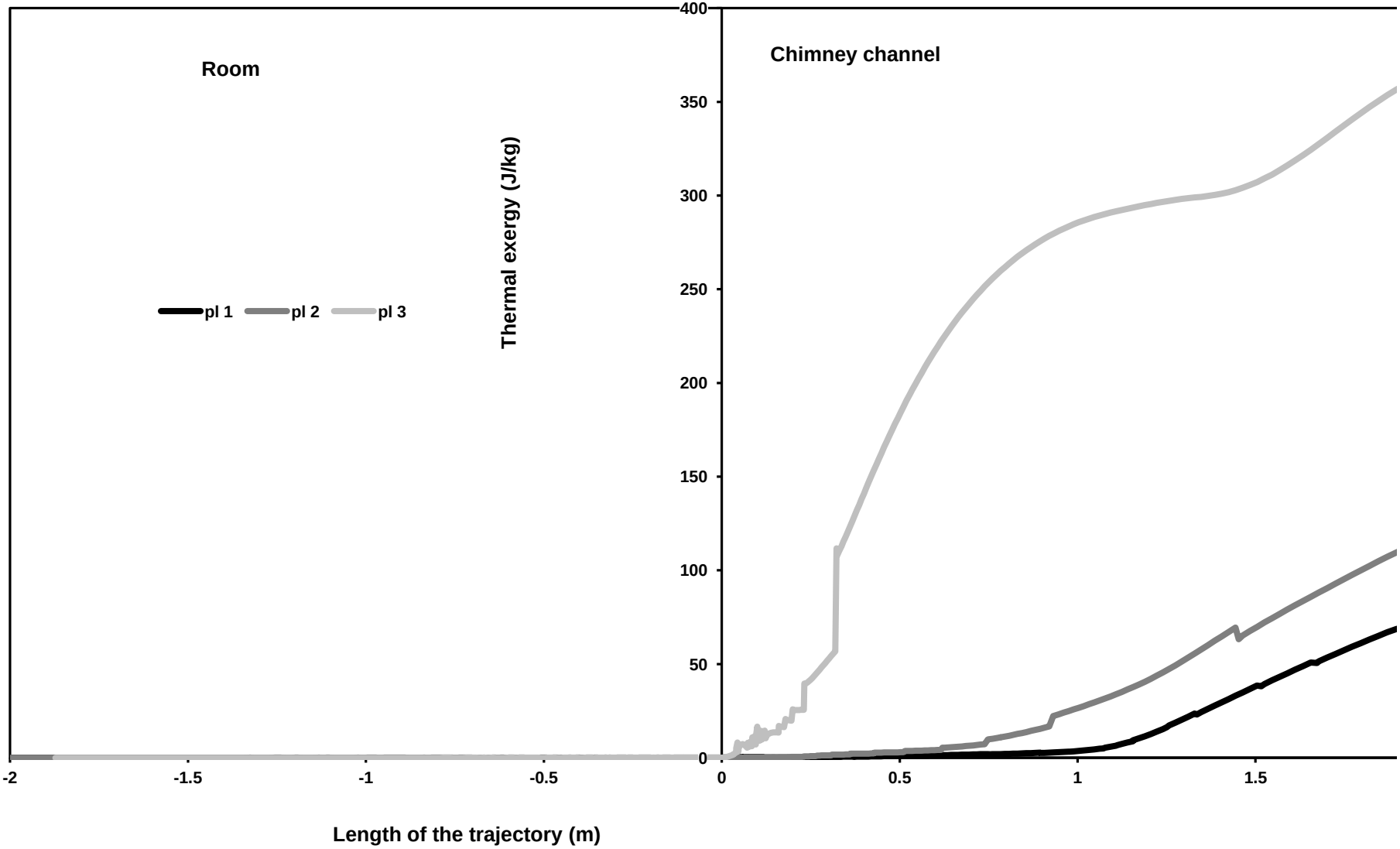
Room
Chimney channel
pl 1
pl 2
pl 3
Thermal exergy (J/kg)
400
350
300
250
200
150
100
50
0
-2
-1.5
-1
-0.5
0
0.5
1
1.5
Length of the trajectory (m)

Figure(s)

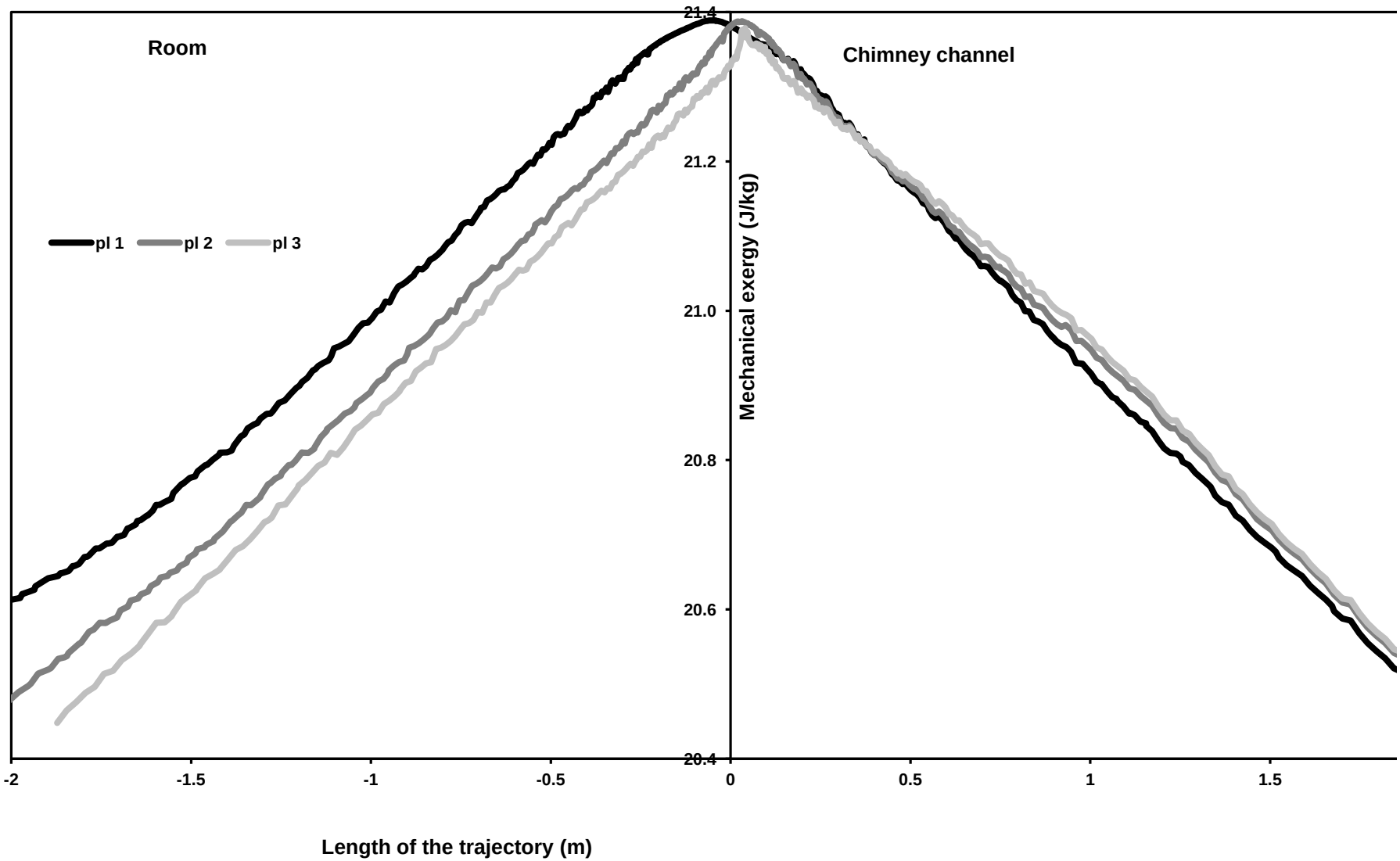
Room
Chimney channel
pl 1
pl 2
pl 3
Mechanical exergy (J/kg)
21.4
21.2
21.0
20.8
20.6
20.4
-2
-1.5
-1
-0.5
0
0.5
1
1.5
Length of the trajectory (m)

Figure(s)

Click here to download high resolution image

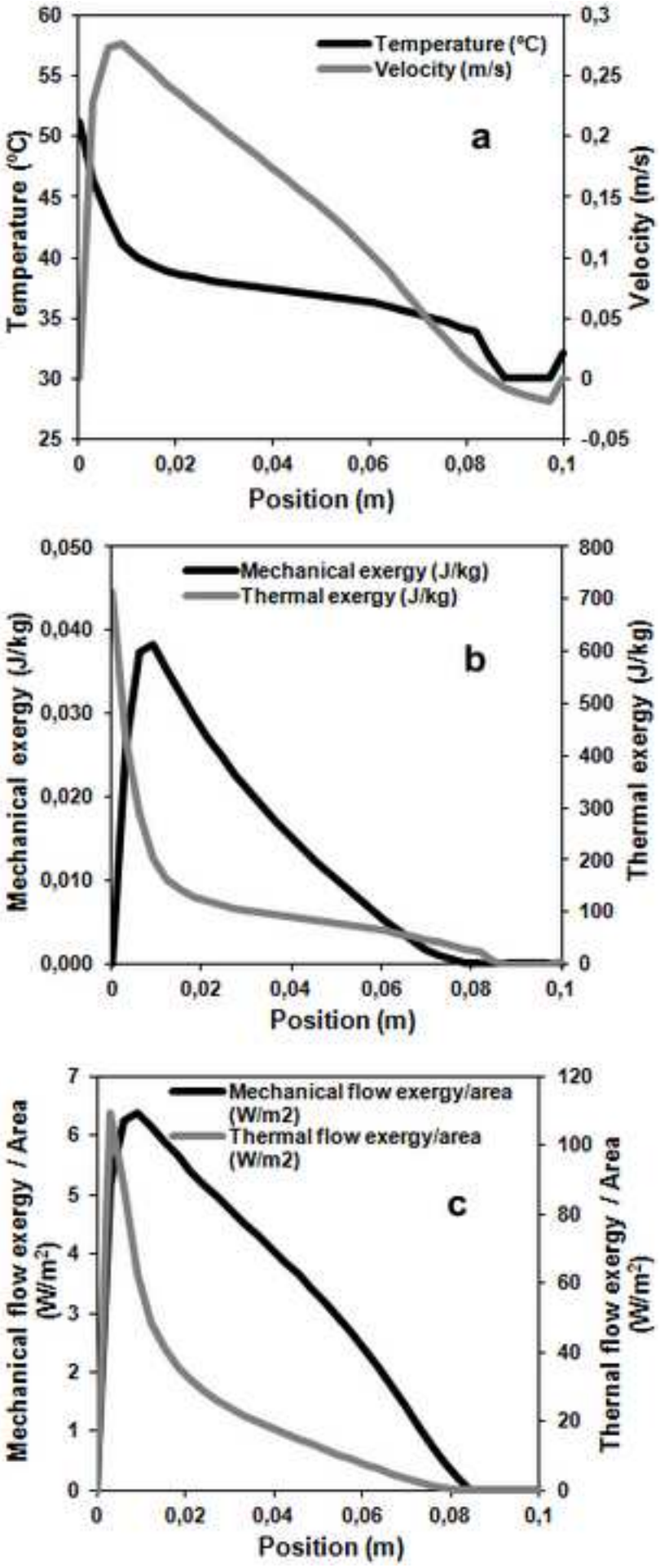

Figure(s)

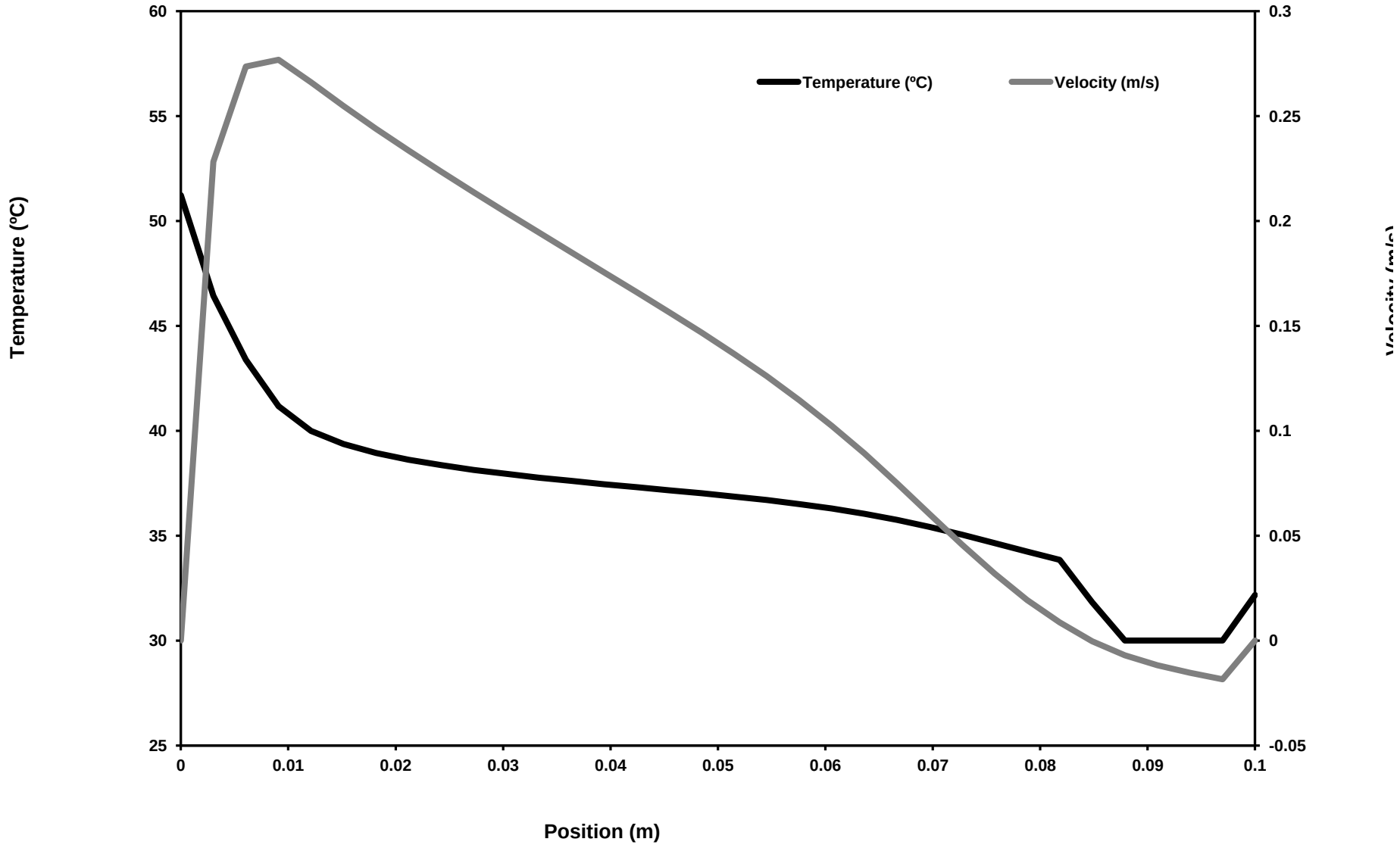
Temperature (ºC)
Velocity (m/s)
60
55
50
45
40
35
30
25
0.3
0.25
0.2
0.15
0.1
0.05
0
-0.05
0
0.01
0.02
0.03
0.04
0.05
0.06
0.07
0.08
0.09
0.1
Position (m)

Figure(s)

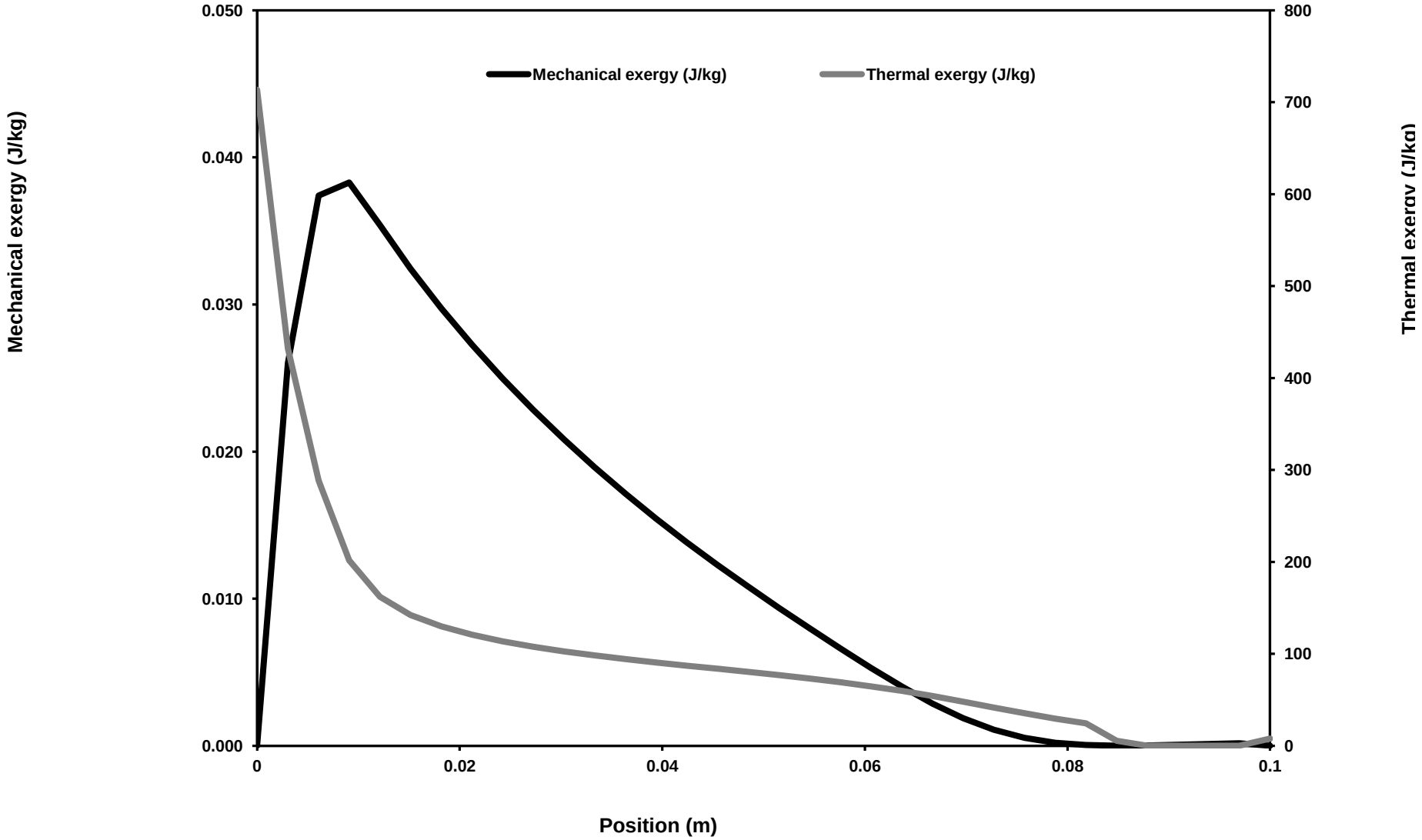
Mechanical exergy (J/kg)
Thermal exergy (J/kg)
0.050
0.040
0.030
0.020
0.010
0.000
800
700
600
500
400
300
200
100
0
0
0.02
0.04
0.06
0.08
0.1
Position (m)

Figure(s)

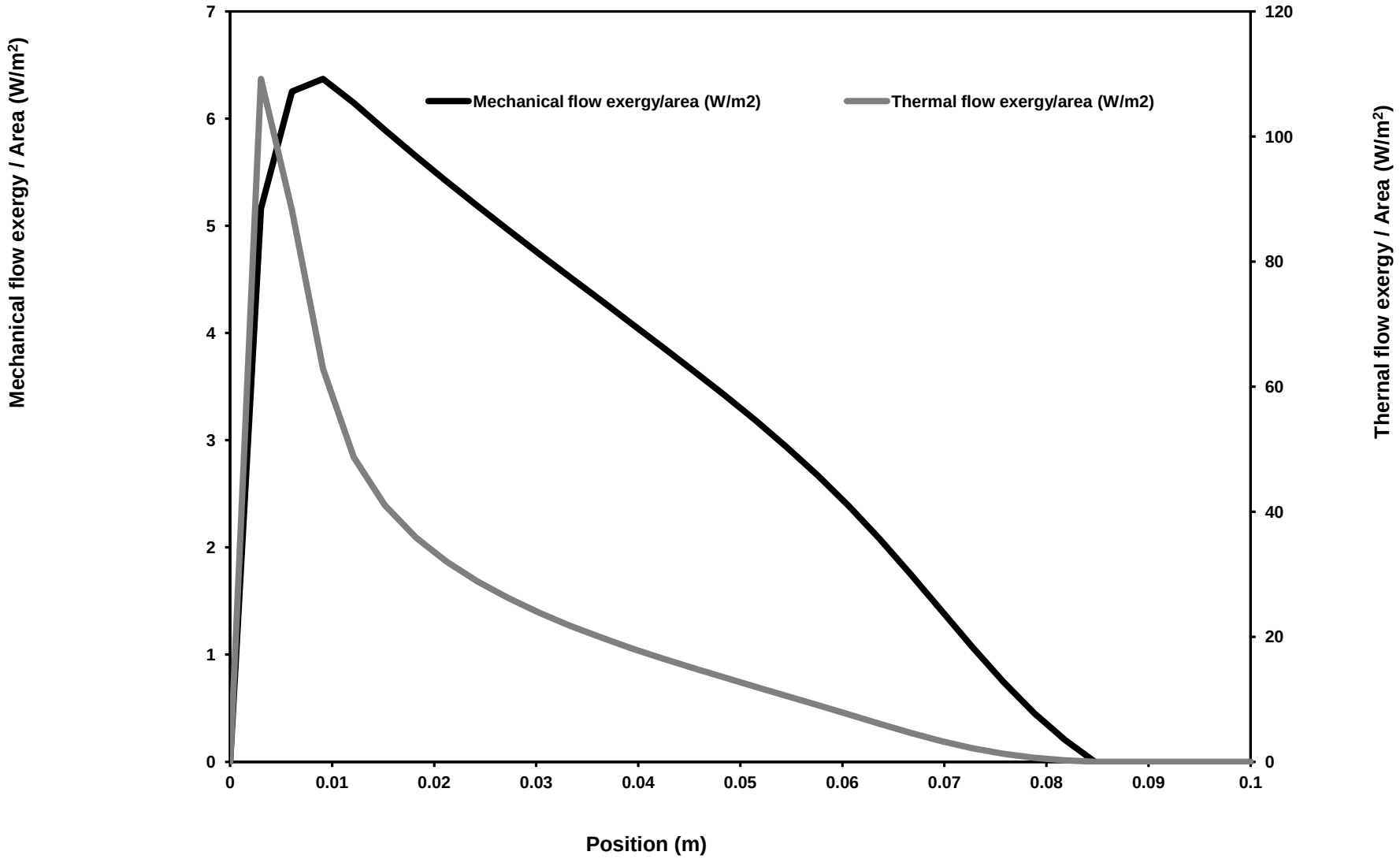
Mechanical flow exergy/area (W/m2)
Thermal flow exergy/area (W/m2)
Mechanical flow exergy / Area (W/m²)
Thermal flow exergy / Area (W/m²)
Position (m)
0
1
2
3
4
5
6
7
0
20
40
60
80
100
120
0
0.01
0.02
0.03
0.04
0.05
0.06
0.07
0.08
0.09
0.1

Figure(s)
Click here to download high resolution image

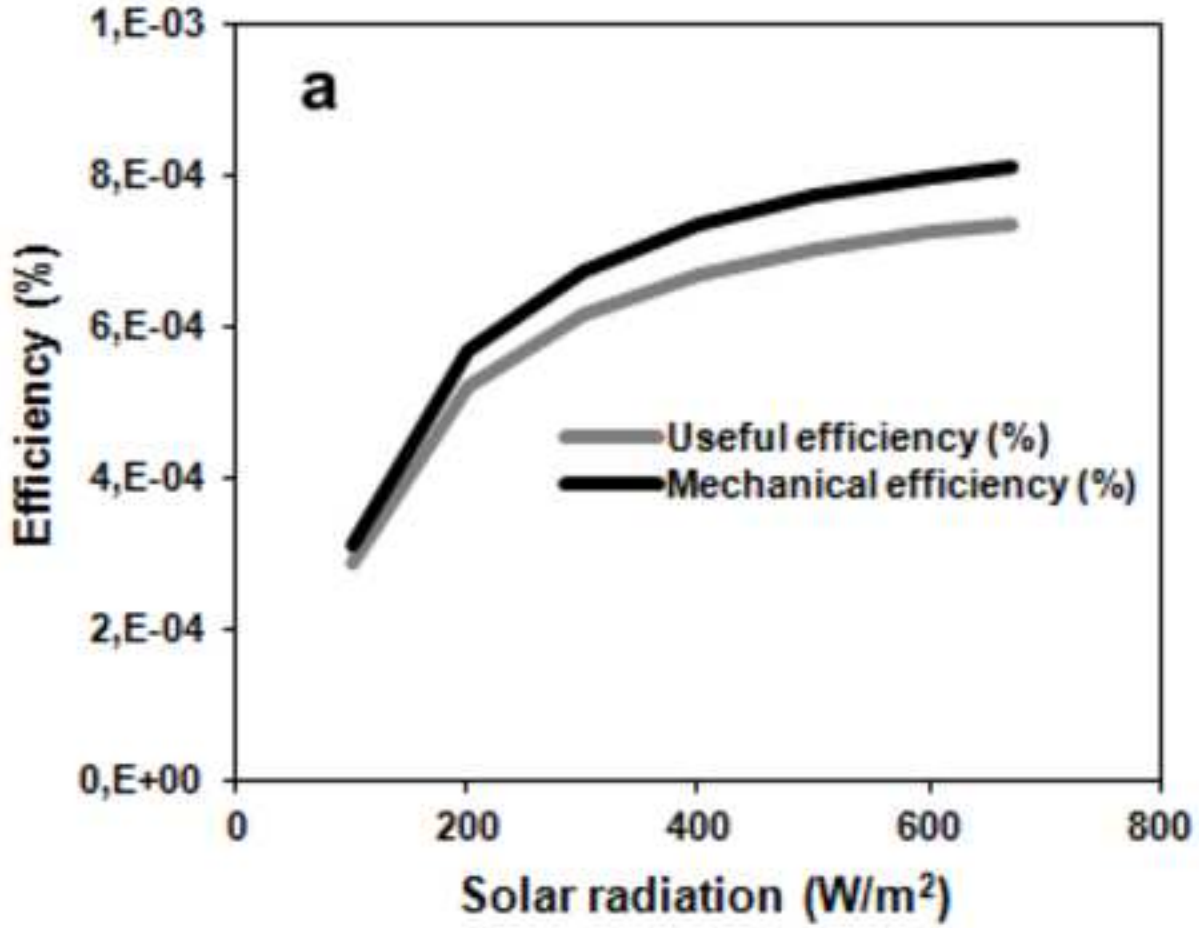

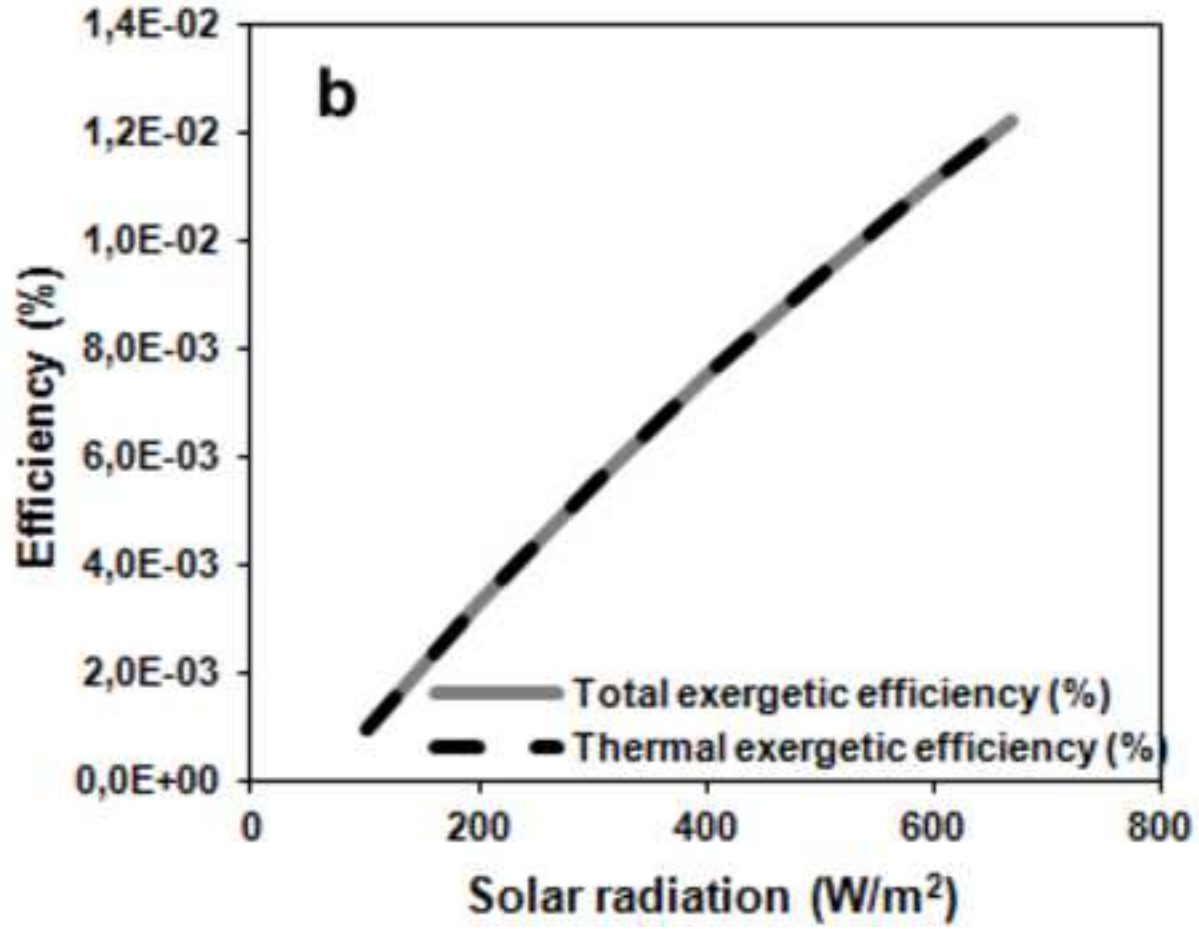

Figure(s)

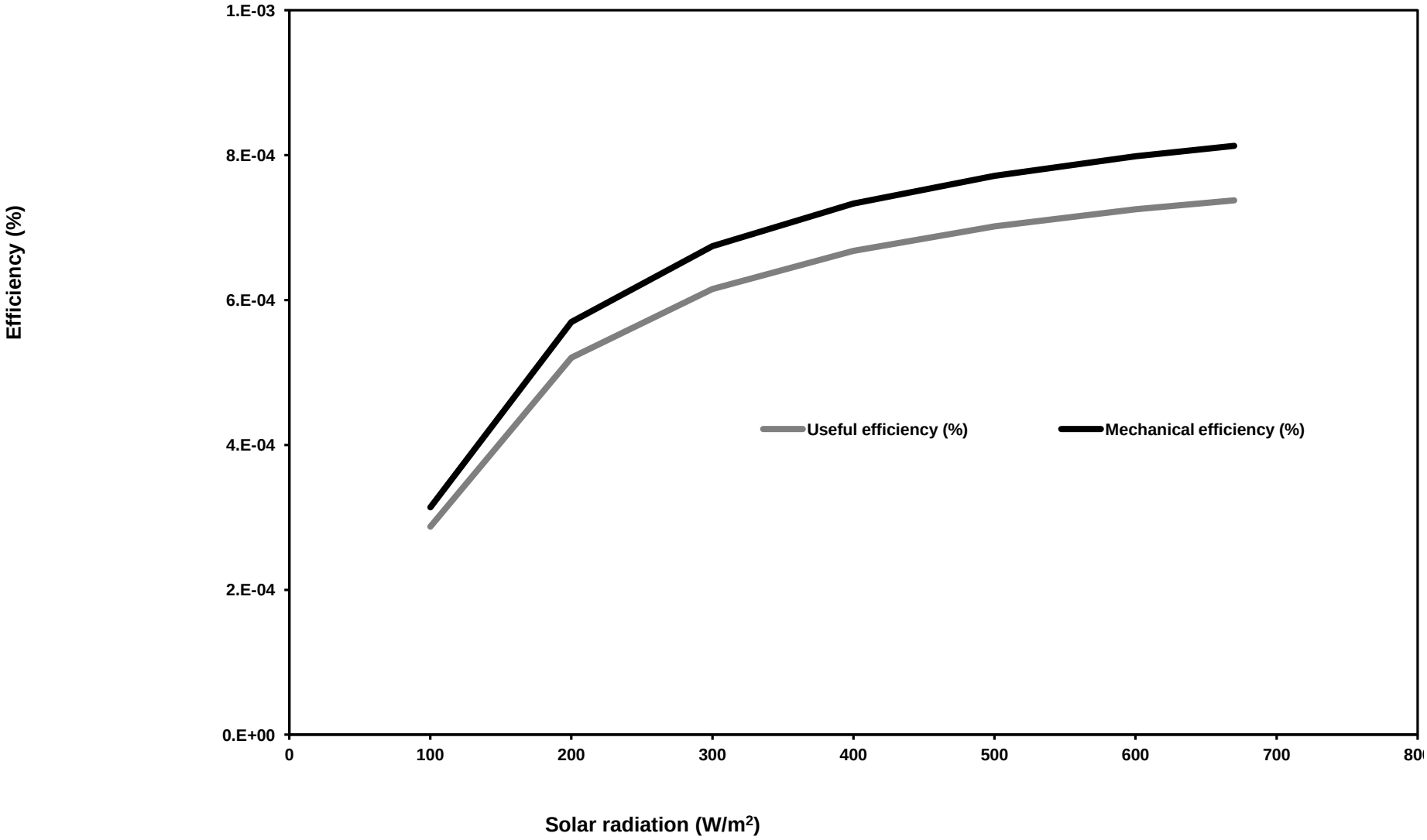
1.E-03
8.E-04
6.E-04
4.E-04
2.E-04
0.E+00
Efficiency (%)
0
100
200
300
400
500
600
700
800
Useful efficiency (%)
Mechanical efficiency (%)
Solar radiation (W/m2)

Figure(s)

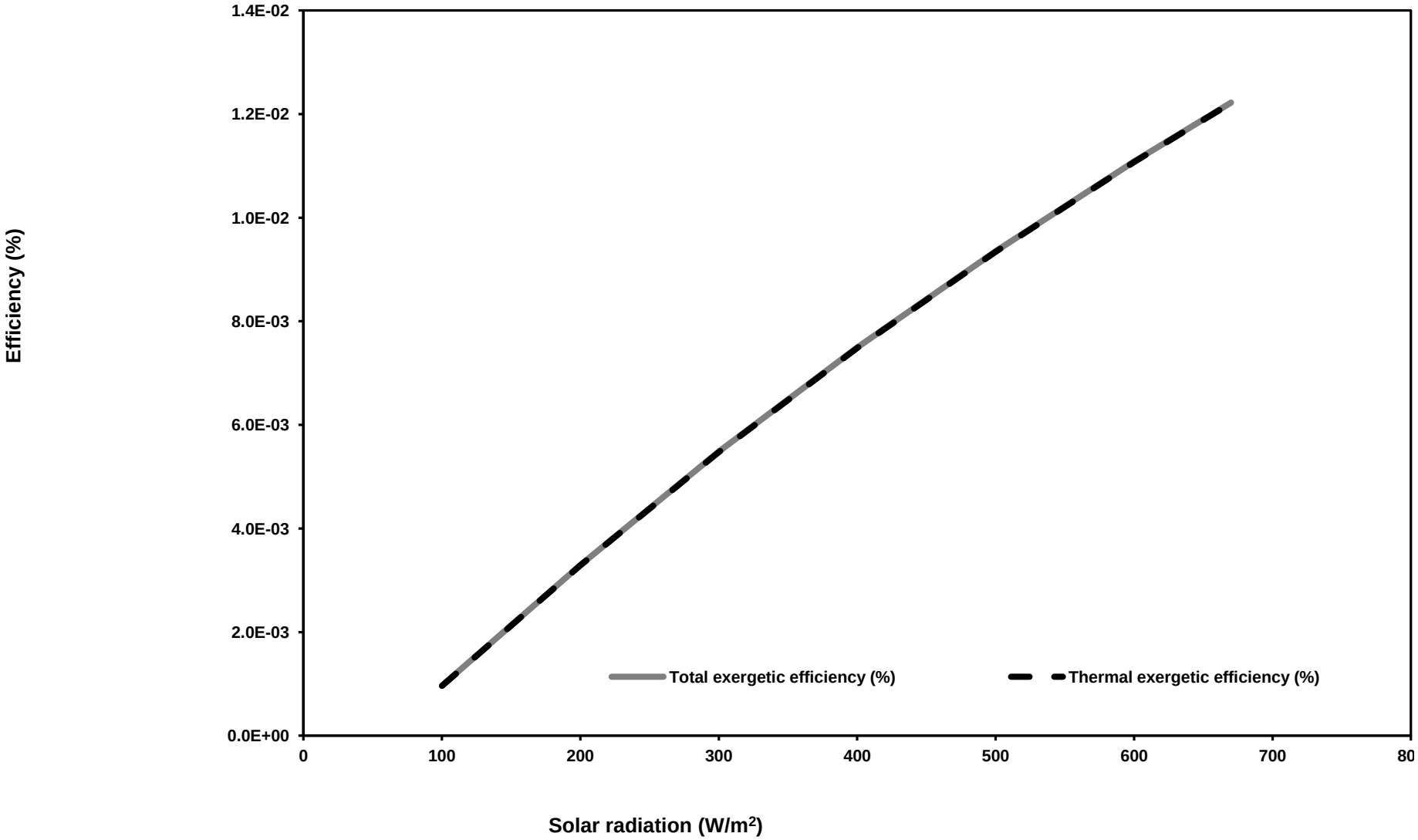
1.4E-02
1.2E-02
1.0E-02
8.0E-03
6.0E-03
4.0E-03
2.0E-03
0.0E+00
Efficiency (%)
0
100
200
300
400
500
600
700
80
Solar radiation (W/m²)
Total exergetic efficiency (%)
Thermal exergetic efficiency (%)